Indian J. Phys. **72B** (5), 427-476 (1998)

REVIEW

IJP B

an international journal

Scattering of electrons and photons by atoms and ions

S N Tiwary

University Department of Physics, BRA Bihar University, Muzaffarpur, Bihar, India

Received 24 February 1998, accepted 4 March 1998

Abstract A review of recent developments in the study of the experimental as well as theoretical elastic and inelastic (excitation, inner-shell excitation which leads to autoionization and ionization processes) scattering of electrons by alkali-metal atoms (Li, Na, K, Rb and Cs) and alkali-like ions (C^{3+}, Fe^{15+}, Ca^{+}, Sr^{+}, and Ba^{+}) in the low, intermediate and high energy ranges is presented, with particular emphasis of the effects of correlation, relativity, exchange, channel couplings and polarization on the various collision processes At low energies, the collision has many of the features of a bound state problem The wave function describing the collision can be accurately represented in terms of a sum of configurations in a similar way to the configuration interaction expansions used for bound state calculations of atoms and ions For the intermediate energies, there should be an infinite number of bound target states and also continuum states should be included in the expansion At low and intermediate energies, the essential physics that must be contained in any accurate calculation of excitation, autoionization and ionization collision cross sections is an adequate configuration interaction description of the target and a scattering approximation that includes distortion of the target by the incident electron, exchange symmetry between the scattered and orbital electrons, coupling to other states of the incident and final states, and correlation effects due to the temporary formation of a compound state of the electron plus target system At high energies, the Born approximation yields excellent results The reason the Born approximation works so well is that the Green function has an inverse energy dependence, so neglecting the kernel is increasingly well justified as the energy increases The energy range of validity of the Born approximation is difficult to determine and depends on the transition of interest and the accuracy required For heavy atoms and ions of high nuclear charge, a relativistic description of the target is appropriate, and in some cases relativistic effects for the colliding electron must be included Many high precision experiments have been performed which need very high accurate theoretical prediction for correct interpretation and identification of different physical effects involved Several powerful sophisticated theoretical methods (*R*-matrix, New *R*-matrix, Close-coupling, Coupled-channel optical, Convergent close-coupling, Distorted wave, Hyperspherical-coordinate, Polarized orbital, Pseudostate, *etc*) have been developed for inclusion of the above mentioned effects which play an extremely important role in order to obtain results of high accuracy for understanding experimental observation of high precision. At present, we do not have a comprehensive and practical atomic scattering theory which accounts for all these effects on an equal footing

A recent theoretical as well as experimental study of a simultaneous ejection of two electrons by a single photon scattering by two-electron systems (He, H^- and H_2) in the low, intermediate and high energy ranges is also reviewed, with particular emphasis on the electronic correlation in the vicinity of the threshold The interaction of a photon with each electron is independent

from the others so that double-photoionization (DPI) is forbidden process unless the electronic correlation is taken into account If two electrons with small kinetic energies leave the residual positive ion, the motion is strongly influenced and controlled by their mutual repulsion due to Coulomb interaction ($1/r_{12}$) The interaction leads to the exchange of energy and angular momentum over long distances and therefore implies a correlation between outgoing electrons. The DPI can be described by the reaction as follows :

$$h\nu + X \rightarrow X^{++} + e + e$$

where X stands for atoms or molecules or ions The initial state wave function can be obtained using configuration interaction (CI) method. The final state consists of a positive ion and two continuum electrons can not be described by CI wave function. Accurate double-continuum wave functions (DCWF) have been a long standing and challenging problem for theorists DCWF can be obtained solving the Schroedinger wave equation for two electrons without imposing any constraint but unfortunately this is not possible For this reason, several existing possible DCWF which are valid in different physical situations will be described At very high incident energies, two ejected electrons are very far away from the residual ion, one can argue that two escaping electrons do not experience Coulomb force Under this situation, one can describe two continuum electrons by a product of two plane waves. A product of two plane waves gives the threshold law which differs from experimental threshold law At intermediate energies, one electron is slow and another fast The slower electron may screen the faster one In this case, one electron can be described by the Coulomb wave function and the faster one by plane wave This also gives the threshold law which disagrees with the experimental law At low energies, one needs fully correlated double-continuum wave function especially in the vicinity of the threshold where electron correlation plays extremely important role in order to obtain accurate results Hyperspherical new R-matrix, Altick asymptotic, distorted wave and product of three Coulomb functions have been used to describe the double-continuum electrons

The validity of existing double-continuum wave functions is analysed and the importance of electronic correlation in both the initial as well as final states wave functions involved in the transition amplitude for double-photoionization process is demonstrated At present, we do not have comprehensive and practical double-continuum wave functions which account the full correlation of two-electron in the continuum Basic difficulties in making accurate theoretical calculations of double-ionization by a single high energy photon especially in the vicinity of the threshold, where the correlation plays an important role, are discussed Illuminating, illustrative and representative examples are presented in order to show the present status and the progress in this field

Future challenges and directions, in reliable electron-atom scattering calculations as well as in high precision double-photoionization cross section calculations, have been discussed and suggested.

Keywords Scattering, electrons and photons, atoms and ions

PACS Nos. : 32 80 Fb, 34.80. Dp

PLAN OF THE ARTICLE

1. Introduction with brief historical review

The beginning of quantitative studies of atomic scattering can be traced back to the Röntgen discovery of X-rays in 1895 [1]. The first study of an electron-atom collision process was the classic experiment of Franck and Hertz [2] in 1911. The first quantum mechanical scattering theory was developed by Born [3] and modified by Oppenheimer [4] for the inclusion of exchange. Ramsauer [5] and Ramsauer and Kollath [6] work on the total scattering cross section of low energy electrons against nobel gases, which contributed so much to the development of quantum theory. Hughes and Rojansky [7], Brinkman and Kramer [8], Bethe [9], Ramsauer and Kollath [10], Massey and Smith [11], and Massey and Mohr [12] developed the atomic collision physics. Around 1935, the growth of scattering process was suddenly retarded by the fast rising interest for nuclear physics. This lack of interest lasted till about 1950 before a few survivors of the old time of atomic physics gave the signal for a new and glorious revival. In 1952, the book by Massey and Burhop [13] appeared on Electronic and Ionic Impact Phenomena. This book provided the basis on which the young generation could start, using the technical tricks developed for nuclear collision physics. These investigations have made important contributions to the growth of physics, both in the development of experimental apparatus and techniques and in the formulation of modern concepts and theory. The continuing and growing interest in the processes by which electrons interact with atoms and atomic ions-elastic scattering, excitation, autoionization, ionization, and recombination—is because these processes play extremely important roles in astronomy, astrophysics, atmospheric physics, laser physics and plasmas of all kinds, from astrophysical plasmas through modest laboratory plasmas to plasmas in controlled fusion research. The modelling of a non-equilibrium plasma requires detailed knowledge of the cross sections for collisions of its components-electrons, photons, atoms, and ions of sequentially higher charge states, depending on the ultimate temperature.

Low energy scattering plays an important role in a number of critical applications. Plasma processing of microelectronic structures promises to be a cost-effective way of increasing component density and hence the speed and capability of a wide range of devices, *e.g.*, in the continued development of plasma etching and plasma deposition important to economic solar cell and high temperature superconductor development. In magnetically confined fusion machines, low temperature plasmas occur near the walls of the device. It is essential to understand how wall materials erode and how the resulting impurities are transported to the central plasma region. It is known that line radiation from incompletely stripped atoms can lead to radiation losses and possible prevention of energy breakeven conditions in a plasma. Similar erosion occurs as spacecraft in low-Earth orbit interact with the uppermost part of the terrestrial

atmosphere, space shuttle glow being a familiar example. The subject of material degradation by interplanetary plasma will become important for longer mission in space. Most emission lines spectra observed in astronomy are produced by electron impact excitation of positive ions and atoms. Electron density and temperature may be deduced from observed intensities of emission lines.

Because of their compelling importance to the modelling and diagnostics of plasmas germane to other fields of science and to the national programs such as defence or controlled fusion, a worldwide resurgence in atomic physics research began in the late 1950. Very significant progress has been made in developing the requisite understanding during the past three decades both experimentally and theoretically, but much remains to be done.

The electron-atom scattering problem is one of the oldest problems in atomic physics, dating back to the early 1900. Through its history, there have been periods for which the problem could be considered solved if one defined solved to mean that agreement between theory and existing experimental data had been attained. However, these periods always ended when new generations of more detailed experiments were performed. In the early days, experiments were designed to measure total cross sections– that is, cross sections summed over electrons spin polarization and atomic magnetic sub-shells and integrated over electron scattering angle. These experiments were interpreted by elementary theoretical calculations – the most notable of which was the highly successful and ever popular plane wave Born approximation (PWBA). However, beginning in the 1960, experimental cross sections differential in the electron scattering angle were reported. These differential cross section measurements represented a major challenge for theorists since the more detailed information could not be explained using the standard elementaries theories. This challenge has become even greater in recent years because of a new generation of experiments which measure the scattered electron in coincidence with emitted atomic photons. In the near future these coincidence experiments will undoubtedly be performed with polarized beams of electrons. The general trend has been for each new level of experimental sophistication to reveal serious shortcomings in previously accepted theoretical methods.

The ultimate goal of any theoretical scattering calculation is to produce accurate scattering amplitudes which could then be used to predict any of the physical observables for the systems. If one wishes to perform quantum mechanical calculations of electron-atom scattering amplitudes, there are two different theoretical methods which may be used – the close-coupling method and the perturbation series method. In the close-coupling method, one expands the scattering wave functions in terms of some complete basis set. This undoubtedly should yield accurate results if a complete basis set could in fact be used. The problem with this method, however, lies in the fact that any appropriate basis set must contain a major contribution from the continuum states which, undoubtedly, must in practice either be ignored or treated in some approximate manner. In the perturbation series method, a series expansion is made for the scattering amplitude. The goal of a perturbation calculation is to choose the series to maximize the rate of convergence of the perturbation expansion. The perturbation series method has the attraction that different physical effects can be more easily isolated and investigated, the various terms have simple interpretations and the leading term is relatively easy to calculate.

It is well known that it is impossible to obtain exact solutions for atomic collision cross sections. In most instances the requisite wave functions are not with complete accuracy, and the approximate wave functions on which we must rely are frequently not orthogonal. Evidently,

as the structural complexity of the colliding systems increases, the difficulty of obtaining good wave functions also increases and more complex reactions become possible. To make matter worse, the structure of the equations to be solved is such that approximate methods must be used even if the necessary wave functions are completely and exactly known, as in the case of the hydrogen atom. The excellent description of electron-atom and electron-atomic ion scattering is given in quantum mechanics [14-19], books [20-35] on atomic collisions and review articles [36-59].

Several standard computer codes[60-66] are available for the electron-atom (ion) scattering. In the present review, we will briefly describe almost all important widely used approximate classical, semiclassical and pure quantum mechanical methods for electron-atom collisions. Some important illuminating, illustrative and representative examples of essential physics will be given for electron-alkali-metal atoms and alkali-like ions scattering. Finally, major conclusions and future directions will be discussed.

2. Scattering of electrons

2.1. Review of approximations

2.1.1. Partial wave method and phase shift

Expansion of the incident plane wave $e^{ik\cdot r}$ in partial waves :

$$e^{ik\cdot r} = \sum_{l=0}^{\infty} (2l+1)\, i^l\, j_l(kr) P_l(\cos\theta), \tag{1}$$

$j_l(kr)$ is the spherical Bessel function and $P_l(\cos\theta)$ is Legendre polynomial.

The scattering amplitude can be written as :

$$f(\theta) = \frac{1}{k} \sum_{l=0}^{\infty} (2l+1) e^{i\delta_l} \sin\delta_l\, P_l(\cos\theta), \tag{2}$$

δ_l is the phase shift and the total cross section

$$\sigma = \int |f|^2\, d\Omega \tag{3}$$

is given by

$$\sigma = \frac{4\pi}{k^2} \sum_{l=0}^{\infty} (2l+1) \sin^2\delta_l, \tag{4}$$

upon using the orthogonality relations for the Legendre polynomials

$$\int P_l(\cos\theta)\, P_{l'}(\cos\theta)\, d(\cos\theta) = \frac{2}{2l+1}\, \delta_{ll'}. \tag{5}$$

Note that σ is a sum of partial cross sections at each l :

$$\sigma = \sum_{l=0}^{\infty} \sigma_l, \quad \sigma_l = \frac{4\pi}{k^2}(2l+1)\sin^2\delta_l. \tag{6}$$

2.1.2. *First Born approximation*

In the first Born approximation, the incident and scattered particles are treated as plane waves $e^{ik_i \cdot r}$ and $e^{ik_f \cdot r}$ that remain undistorted by the interaction. Only forward $i \rightarrow f$ transition between the initial and final states i and f are considered and for electron impact, electron exchange and spin effects are not taken into account. A single equation provides the solution to the scattering problem, no coupled equations are involved. The first Born approximation is valid for high energy, but accurate cross section can be obtained by its use only if accurate wave function for the stationary states of the colliding structure are available. At low energies, the first Born approximation generally overestimates the cross section.

To show how we can obtain higher order Born approximation, we shall develop the Born series, or expansions, displaying the results in modern Dirac notation, which makes the underlying physics more transparent. Consider the simplest situation of structureless projectiles being scattered by a static potential $U(r)$. We solve the integral equation by iteration, starting with the incident plane wave $\Phi_{k_i}(r) = e^{ik_i \cdot r}$ as the zero order approximation and obtain

$$\Psi_{k_i}(r) = \Phi_{k_i}(r) + \int G_0^+(k, r, r') U(r') \Phi_{k_i}(r') dr'$$

$$+ \int\int G_0^+(k, r, r') U(r') G_0^+(k, r', r'') \Phi_{k_i}(r'') dr' dr'' + \ldots . \quad (7)$$

Writing this Born series as shown implies an assumption that the sequence of term converges toward the exact wave function. The function G_0^+ is the outgoing Green function

$$G_0^+(k, r, r') = -\frac{1}{4\pi} \frac{e^{ik|r-r'|}}{|r-r'|} . \quad (8)$$

The corresponding Born series for the scattering amplitude is

$$f = -\frac{1}{4\pi} < \Phi_{k_f} | U + UG_0^+ U + UG_0^+ UG_0^+ U + \ldots | \Phi_{k_i} > . \quad (9)$$

Here Φ_{k_f} is the final plane wave function. The first term in this series is

$$f_{B1} = -\frac{1}{4\pi} < \Phi_{k_f} | U | \Phi_{k_i} > = -\frac{1}{4\pi} \int e^{ik \cdot r} U(r) dr, \quad (10)$$

the first Born approximation to the scattering amplitude. The second Born approximation consists of the sum of the first two terms, and so on. The series that we have obtained here are perturbation expansion in powers of the potential.

k is the momentum transferred during the collision, *i.e.*, $k = k_i - k_f$. The scattering amplitude in the first Born approximation also applies to inelastic collisions if a multiplicative factor $\frac{k_f}{k_i}$ is introduced into these forms.

2.1.3. *Bethe-Born approximation*

In 1930, H. A. Bethe [9] proposed a modification of the Born approximation in which he made the additional assumption that the product of the momentum transfer and the range of interaction is small. Then the exponential term in the first Born approximation for the scattered amplitude

can be expanded and the integration carried out term by term. A series of terms corresponding to the atomic transition moments is obtained.

2.1.4. *Coulomb-Born approximation*

The approximation is useful in describing collisions of electrons and ions with target ions, in which the Coulomb interaction of the projectile with the target nucleus can be important. The Born plane wave functions are replaced by Coulomb wave functions corresponding to the nuclear charge. For highly charged ions, the long range Coulomb interaction is dominant, and all other interaction can be treated as small perturbations. The Coulomb-Born approximation (CBA) is never good for electron-neutral scattering. It is better, comparatively speaking, for electron-ion collisions than is the Born approximation for electron-neutral collisions.

2.1.5. *Versions of the Born approximation that include electron exchange*

The first attempt to account for electron exchange was made by Oppenheimer[4]. He made the same basic as used in the Born approximation but his method of calculation the exchange amplitude is much less satisfactory than the Born approximation for the direct scattering amplitude mainly because in the Born-Oppenheimer approximation the initial and final states are not orthogonal. The result is that the addition of any constant to the interaction potential gives a nonzero change. The Born-Oppenheimer (BO) approximation tends to overestimate the cross sections to an excessive degree. An improvement was made by Ochkur, who suggested that for g should be regarded as an expansion in inverse powers of the impact energy, with the result that g is expressed in term of the direct amplitude f. Then, only the first term should be retained because higher term would cause the result to diverge at lower energies. The Ochkur approximation to the exchange integral is a good approximation only at impact energies high enough for the integral to be small. According to Massey and Burhop, any success that the Born-Ochkur approximation may have at low energies in improving the agreement between theory and experiment must be regarded as empirical. In the Born exchange approximation, the exchange scattering amplitude is related to the direct scattering amplitude by the equation (Massey and Burhop)[13].

$$g(k', k) = f(k, k') = e^{i\delta(k,k')} f_B(k, k'), \tag{11}$$

$$f(k', k) = f_B(k', k), \tag{12}$$

where f_B is the usual Born approximation to the direct scattered amplitude. Here $e^{i\delta}$ is an arbitrary phase factor, it is difficult to know which value of δ to choose. This method does not suffer from nonorthogonality difficulties, but it does suffer from all the shortcomings of the Born approximation. Tiwary and his coworkers[67-85] have performed extensive investigations for the electron-atom (ion) scattering employing several theoretical methods as well as discussed several modifications suggested by Ochkur and Vainshtein *et al.*

2.1.6. *Quantal impulse (sudden) approximation*

This approximation, introduced by Fermi, describes a many-body scattering problem in terms of known two-body scattering amplitudes. The underlying idea can be illustrated in terms of the scattering of a structureless projectile (1) by a hydrogen atom, the nucleus being labeled (2) and the orbital electron (3). The Hamiltonian for the system is

$$H = H_0 + V_{12} + V_{13} + V_{23}, \tag{13}$$

where H_0 is the sum of the kinetic energy operators. We now attack the problem by assuming that the collision of the projectile with the orbital electron takes place as if the electron is free except for having a momentum probability distribution that is determined by its interaction with the nucleus. Thus we are assuming that apart from determining the momentum distribution of the bound electron. V_{23} has little effect and can be ignored in the cattering calculation. Another statement of the basic assumption is that the collision between the projectile and the electron is sudden (*i.e.*, the collision time is small compared with the characteristic period of the orbital motion of the electron). One would expect the impulse approximation to be useful when (1) the impact energy greatly exceeds the binding energy of the target particle being considered and (2) the reduced wavelength of the relative motion of the projectile and target system is much smaller than the mean separations of the particles of the target.

2.1.7. *Distorted wave approximation*

This starting point for the discussion of this approximation is the infinite set of coupled differential equations, derived for the excitation of hydrogen atoms by electron impact but capable of being generalized to more complex systems and other collisions. These equations may be solved in the Born approximation by representing the incident beam electron by an undistorted plane wave

$$F_0(r) = e^{ik_0 r} \tag{14}$$

and taking the interaction matrix elements V_{nm} and V_{mn} to be zero except for $m = 0$, where 0 designates the initial state and n the final state of the system. As the relative impact velocity decreases, we try to improve this approximation by considering more terms. The distorted wave (DW), or distortion, approximation ignores transitions through intermediate states (as does the Born) but takes account of the distortion of the incident and scattered waves by the static field of the target. The distortion is allowed for by the retaining the matrix elements V_{nn} and V_{00}, and the transition occurs via V, all other elements are set equal to zero. The infinite set of equations then reduces to the pair of equations :

$$\left[\nabla^2 + k_0^2 - \frac{2m}{\hbar^2} V_{00}\right] F_0 = \frac{2m}{\hbar^2} V_{0n} F_n , \tag{15}$$

$$\left[\nabla^2 + k_n^2 - \frac{2m}{\hbar^2} V_{nn}\right] F_n = \frac{2m}{\hbar^2} V_{0n} F_0 . \tag{16}$$

The neglect of $V_{nn}F_n$ is valid when F_n is much smaller than F_0 (weak coupling). This approximation may not be justified, however, if the matrix element V_{0n} becomes large, producing strong coupling between (15) and (16). If weak coupling is assumed, the first equation may be solved to give a function with asymptotic form

$$F_0 \sim e^{ik_0 z} + r^{-1} e^{ik_0 r} f_0(\theta) . \tag{17}$$

When this solution is put into the second equation, a solution is found for it with asymptotic form

$$F_n \sim r^{-1} e^{ik_n r} f_n(\theta) . \tag{18}$$

The function is equation (17) represents the incident particle. It corresponds to a distorted wave with the asymptotic form of a plane wave plus an outgoing spherical wave. The scattered

particle is represented by a distorted wave function with the asymptotic form of an outgoing spherical wave.

2.1.8. *Perturbed stationary state and perturbed rotating atom approximations*

The number of matrix elements that are important in the description of the interaction between colliding systems generally increases rapidly as the relative impact velocity decreases, so that the use of the distorted wave or second Born approximation does not permit reliable calculations to be made at much lower velocities than does the first Born approximation. It is evident that slow collisions can not be treated accurately by expanding the wave function of the systems in terms of the eigenfunctions of the isolated target, but Mott suggested that it might be legitimate to perform the expansion in terms of the eigen functions that would describe the quasi-molecule formed by the colliding structure if their relative position vector were momentarily fixed in space. This assumption is equivalent to what is frequently called the perturbed stationary state (PSS) approximation. It allows for the gradual nature of the collision in the near-adiabatic region by treating the kinetic energy of relative motion as a perturbation.

The PSS approximation is rarely an adequate approximation except for symmetric resonance charge transfer. For other reactions at any given impact velocity, collisions at sufficiently small impact parameters generally are not nearly adiabatic, as assumed, because of the rapid rotation of the internuclear axis, and these close impacts normally give the dominant contribution to the calculated cross section at low energies. However, close encounters make only a small contribution to the cross section for symmetric resonance charge transfer at low velocities, because the probability of this reaction is high up to very large values of the impact parameter.

2.1.9. *Polarized orbital approximation*

As we have seen, one approach to the calculation of collision cross sections is to expand the scattering wave function in an appropriate set of basis functions and then truncate this set, so that only a finite set of coupled equations has to be solved. A different approach is provided for slow electron scattering by the polarized orbital method. It attempts to incorporate the essential physics of scattering into the form of the wave function. The projectile, as it approaches the target, induces electric multipole moments in it, and these moments affect the motion of the projectile. In this method, only the effect of the dipole moment is acknowledged. This fact prompts the choice of a trial wave function for electron-atom collision, of the form

$$\Psi^{I} = (1 \pm P_{12})[\Psi_0 (r_2) + \phi_0 (r_1, r_2)]\, F_0(r_1), \tag{19}$$

where $\Psi_0 (r_2)$ is the original, unperturbed wave function of the target, $\phi_0 (r_1, r_2)$ gives the polarization of the target during the collision, and $F_0(r_1)$ is the wave function of the projectile P_{12} is the exchange operator that interchanges electrons 1 and 2. The functions $\varphi_0 (r_1, r_2)$ can be calculated by perturbation theory using the electrostatic dipole perturbation, and then one can calculate an effective polarization potential in which the projectile is to move. We see that the polarized orbital approximation takes into account both the effect of polarization and the effect of exchange in a relatively simple fashion. If the distortion exchange terms in the polarized orbital analysis are set equal to zero, we obtain the exchange adiabatic approximation. Without exchange, we have the adiabatic approximation, which merely states that the electrostatic potential describing the interaction between projectile and the target varies so slowly that the

target electrons can smoothly adjust to the disturbance. Mathematically, the kinetic energy of the projectile is to be neglected.

2.1.10. *Close-coupling approximation*

Here the wave function for the system of projectile plus target is expanded in terms of the complete set of eigenfunctions (assumed known) of the target Hamiltonian. For a structureless projectile colliding with an N-electron atom, we could write

$$\Phi(r_1, r_2) = A\sum_{\gamma} F_{\gamma}(r_1)\,\varphi_0(\gamma, r_2), \tag{20}$$

where r_1 represents the spatial and spin coordinates of the projectile and r_2 the coordinates of the atomic electrons. Any possible combination of the good quantum numbers belonging to the total system is denoted by γ. The symbol A implies antisymmetrization of the total wave function. The expansion coefficient F describes the radial motion of the projectile relative to the target in its various quantum states in the close-coupling approximation, only a relatively small number of channels are retained. Some of the open channels and closed channels should be included. The radial partial wave scattering functions F satisfy a set of M coupled integrodifferential equations of the form

$$\left[\frac{d^2}{dr^2} + k_i^2 - \frac{l_i(l_i+1)}{r^2}\frac{\hbar^2}{2m}\right]F_i(r) = \sum_{j=1}^{M} V_{ij}(r)\,F_j(r) + \int_0^{\infty} W_{ij}(r, r')\,F_j(r')dr', \tag{21}$$

where V_{ij} is a direct electron-electron plus electron-nucleus potential, and W_{ij} is the exchange kernel. The r refer to the exchanged electrons. These close-coupling equations can give accurate cross sections provided that, in the spirit of perturbation theory or bound states, all of the target states lying close to the initial and final states in energy are included. However, the slow convergence of the truncated expansion makes close coupling calculations intractable at higher impact energies, at which more states are accessible and more angular momenta become important. Also, it is virtually impossible to apply the method to scattering from excited states, since close spacing of the excited levels requires that a large number of states be included in the expansion. Finally, the large number of angular momenta involved in heavy particle collisions makes the close-coupling method infeasible for this important class of collisions. The method is, however, effectively exact in the prediction of the positions and shapes of threshold effects and resonances in low energy collisions of electrons with ground state atoms.

2.1.11 *Static exchange approximation*

When considering the elastic scattering of electrons, the use of only the first term in (20) is a good approximation provided that the coupling between the target ground state and its other bound and continuum states is weak. This static exchange approximation is tantamount to assuming that the target remains undistorted during the collision and that no virtual transitions to excited states take place. The wave functions for the e-H elastic scattering problem are written as

$$\Psi_{\pm}(r_1, r_2) = F_1^{\pm}(r_1)\,\Psi_1(r_2) \pm F_1^{\pm}(r_2)\,\Psi_1(r_1) \tag{22}$$

The spatial part of the wave function must be either symmetrical (Ψ_+) or antisymmetrical (Ψ_-) with respect to the interchange of the electrons. These functions correspond to the singlet

spin state ($S = 0$) and the triplet spin state ($S = 1$), respectively. The function F_1 satisfy the equation

$$(\nabla_1^2 + k_1^2)\, F_1^{\pm}(r_1) = 2V_{11}(r_1)\, F_1^{\pm}(r_1) \pm 2 \int K_{11}(r_1, r_2) F_1^{\pm}(r_2)\, dr_2, \tag{23}$$

where

$$V_{11}(r_1) = \langle \Psi_1 \left| -\frac{e^2}{r_1} + \frac{e^2}{|r_1 - r_2|} \right| \Psi_1 \rangle \tag{24}$$

is the static (direct) part of the effective potential and

$$K_{11}(r_1, r_2) = \Psi_1^*(r_1)\, \Psi_1(r_2) \left[\frac{e^2}{|r_1 - r_2|} - (E_{total} - 2E_1) \right] \tag{25}$$

is the exchange part. The direct potential V_{11} is the electrostatic energy associated with the projectile and the undistorted hydrogen atom, averaged over Ψ_1, and K_{11} is a non-local exchange potential.

2.1.12. *Pseudostate approximation*

Computational difficulties increase rapidly with the number of target eigenfunctions used in the close-coupling expansions, in practice, only a few bound states and continuum states are included. One partial remedy for this shortcoming is to add to the approximate wave function in the truncated functions of the form $\phi_n(r_2)\, F_n(r_1)$, where ϕ_n is not a target eigenfunction but rather a function chosen to represent some appropriate average of bound and continuum states. The states thus introduced are fictitious, not real, and for this reason, they are called pseudostates. There is no unique way in which to choose the pseudostates to be used, although questions of normalization and orthogonality need to be addressed. The inclusion of pseudostates helps offset one of the effects of truncation the eigenfunction expansion, namely, the loss of flux from the open channels in the expansion to the remaining open channels. Incidentally, another effect to the truncation of the expansion is the loss of terms that contribute to the description of the distortion of the target. The defect is remedied by adding terms of the type used in the polarized orbital approximation. The pseudostates can introduce spurious thresholds as resonances and these artifacts can lead to inaccuracies in computed cross sections.

2.1.13. *Correlation approximation*

First, some background information, which is presented in much more detail by Weiss [86]. In the independent particle model of the atom, the states of the atom is described by a single configuration, each electron being assigned to some one-electron wave function, or orbital. The wave function for the entire atom is then taken to be an antisymmetrized product of orbitals, with the population of the orbitals determined by Bohr Aufbau Principle. For a closed shell atom, the wave function is a single determinant formed from the product of the single particle orbitals and spin functions. In general, the wave function for the excited states and open shells is a linear combination determinants that gives a pure LS state (*i.e.*, one that is simultaneously an eigenfunction of the operators L^2 and S^2. The Hartree-Fock (HF) approximation

is the variational formulation of the independent particle model of the atom. Correlation energy is the difference between the HF value of the total energy of the atom and the exact energy. The term correlation thus relates to the error in the HF model, which represents the effect of the electrons on each other in an average way without concern for the detailed fashion in which the electronic motions are correlated. Correlation effects may be calculated by the method of configuration interaction (CI) or the technique of superposition of configurations (SOC). When the initial and final states of the target are not well separated in energy from all other states, then the close-coupling approximation often converges only slowly. An effective stratagem may be to add a series of term involving power of the interelectron distance r_{ij} to a close-coupling expansion that already includes the states of crucial importance. Thus correlation effects are explicitly introduced into the wave function. This technique is the correlation approximation. The added terms usually involve square integrable N + 1 electron function known as L^2 functions. Tiwary and his collaborators [87-107] have extensively studied the effects of correlation, relativity, quantum electrodynamic (QED), finite nuclear size (FNS) and parity non-conservation (PNC) in alkali-metal atoms and alkali-like ions.

2.1.14. *Closure approximation*

We can illustrate the essential feature of this approximation by considering a specific calculation as outlined by Walters. He starts with the second Born term for the transition $0 \rightarrow f$

$$f_0^{B_2} = -\frac{1}{8\pi^4} \sum_n lim_{\eta \to 0^+} \int dk \frac{< k_f \Psi_f |V| k \Psi_n > < k \Psi_n |V| k_0 \Psi_0 >}{k_n^2 - k^2 + i\eta} . \qquad (26)$$

where atomic units are used. The sum over intermediate states Ψ_n poses a serious problem because it covers all bound and all continuum states of target. However, if the intermediate states are all assigned an average energy is replaced by

$$\overline{k^2} = k_0^2 + (\varepsilon_0 - \bar{\varepsilon}) , \qquad (27)$$

which is independent of n. Then all eigenfunction Ψ_n, and the completeness of the set of states can be utilized :

$$\sum_n |\Psi_n > < \Psi_n| = 1 . \qquad (28)$$

The trivial evaluation of the sum then provides the approximation

$$\overline{f_0^{B_2}} = -\frac{1}{8\pi^4} \sum_n lim_{\eta \to 0^+} \int dk \frac{< k_f \Psi_f |V| k > < k |V| k_0 \Psi_0 >}{k^2 - k^2 + i\eta} . \qquad (29)$$

This closure approximation was first used by Massey and Mohr. Their choice of $\varepsilon = \varepsilon_0$ led to serious problems, the approximation can be improved by evaluating explicitly a few of the terms with their exact energies and using an average for the remainder. This matter is discussed by Walters.

2.1.15. *Quantum defect method*

Let us consider the scattering of an electron in a modified Coulomb field, one that has the asymptotic form $-Ze^2/r$ but that deviates from the Coulomb form at small r. There is an infinite

discrete set of bound states for each value of l. We can classify these states in terms of the limit to which they pass if the field becomes purely Coulombic for all r. We can write for the energy of a state

$$E_{nl} = -\frac{2\pi^2 me^4 Z^2}{\nu_{nl}^2 h^2}, \tag{30}$$

Where $\nu_{nl} = n - \mu_{nl}$. The quantity μ_{nl} is called the quantum defect, it varies slowly with energy and tends to zero in the limit of a pure Coulomb field. The quantum defect method for atomic collisions originated with Seaton. One of its useful aspects is that it provides a relation between the cross section for the l-th partial wave and the quantum defect $\mu_l(k^2)$, considered and extrapolated to positive energies.

$$\cot \sigma_l (k^2) = (1 - e^{\frac{\pi\beta}{k}}) \cot \pi\mu_l (k^2) \tag{31}$$

where

$$\frac{\beta^2}{4\nu_{nl}^2} = \frac{8\pi^2 mE_n}{h^2} \tag{32}$$

The quantum defect method has proved valuable in the calculation of cross sections electron-positive ion collisions. In the limit $k^2 \to 0$

$$\eta_l = \pi\mu_l \tag{33}$$

so that if the bound state energies are known from spectroscopic observations, we can obtain the phase shift, and thus the cross section, with very little effort. Seaton has developed a multichannel quantum defect method, which is a generalization of the single-channel method

2.1.16. R-matrix method

The R-matrix method was introduced by Wigner [108] in the context of nuclear physics. It has been subsequently developed by Burke and his co-workers [109-110] for the study of collisions of electrons with atoms and ions. This method is meeting with considerable success in a variety of types of electron-molecule collisions, including elastic, vibrational excitation, electronic, and dissociative attachment. The reactance (R) matrix is related to the scattering (S) matrix by the equation

$$S = (1 + iR)(1 - iR)^{-1}. \tag{34}$$

The R-matrix is Hermitian, and the potential describing the scattering is real, the elements R_{ij} are real and the matrix is symmetric. It is frequently advantageous to work with R rather than S because the R_{ij} are real. Furthermore, any approximation to R that preserves the symmetry of the matrix ensures that S is unitary and hence that the number of particles in the system is conserved.

In this method configuration space is divided into two regions as shown in Figure 1. For the scattering of electrons from an atom, exchange can be neglected outside some radius a. Hence for $r > a$, the collision is described by coupled differential (rather than integrodifferential) equations that often have analytical solutions easily obtainable by numerical method. The basic problem, then, is to calculate the R-matrix in the internal region ($r < a$). The S matrix and

cross section can then be obtained from the R-matrix through the solution in the external region. The K and T matrices can be obtained from the S matrix. The collision cross section can be calculated from the T matrix.

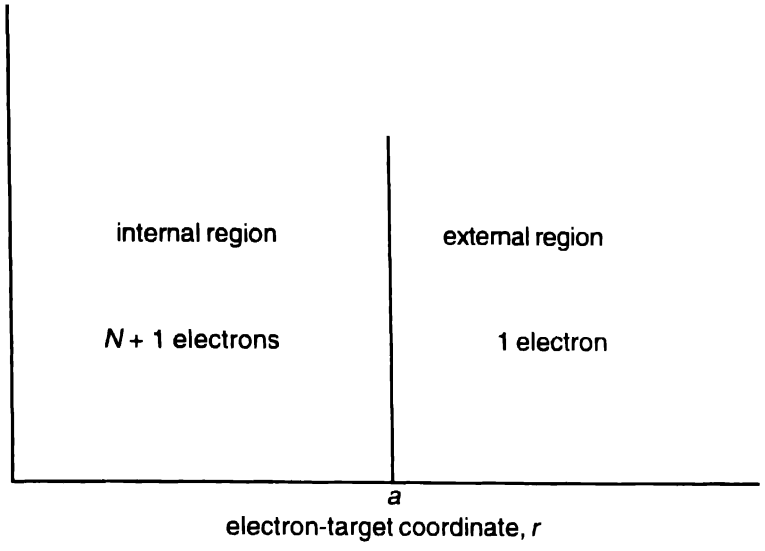

Figure 1. Partitioning of configuration space in the conventional R-matrix method (Ref. 110)

2.1 17. New R-Matrix method[*]

The partitioning of configuration space in the new R-matrix approach is shown in Figure 2. In comparing this partitioning with that illustrated in Figure 1 adopted in the usual R-matrix

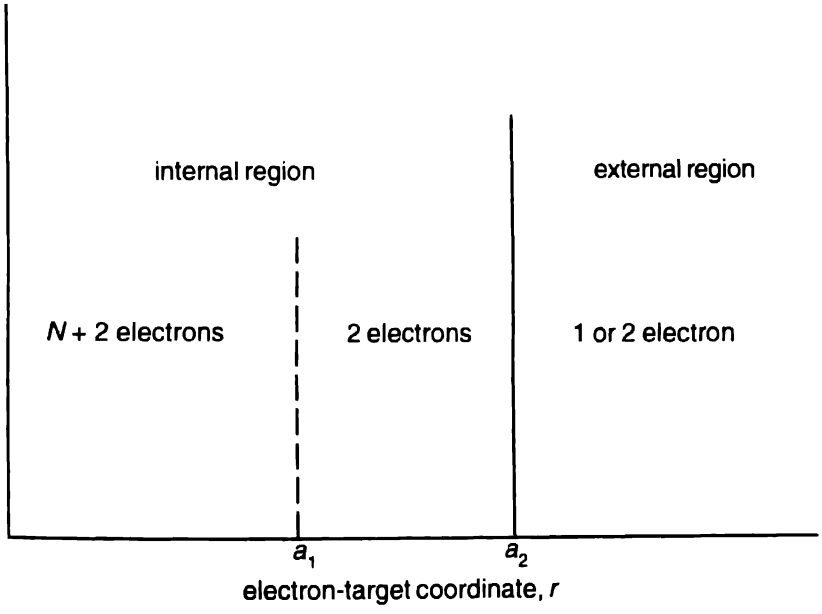

Figure 2. Partitioning of configuration space in the new R-matrix method (Ref. 110)

method we see that the internal subregion is chosen to just envelope the charge distribution of the target states of the N-electron ion core retained in the representation of (2).

In this subregion electron exchange and correlation effects between both continuum electrons and the N-electron core are included and in the case of molecular targets, a multicentre wave function is appropriate. The radius a_2 of the outer subregion is chosen to just envelope the charge $(N+1)$ electron target retained in the representation of (3). In this subregion, only the outer valence electron of the target in (3) and the scattered electron are present and the interaction between these two electrons in the field of the residual ion is included. Also in this subregion both these electrons can be represented by single centre wave functions. In practice, a_2 can be much larger than a_1 because the orbitals representing the target states in (2) are usually of much shorter range than the valence orbitals representing the target states in (3) Finally, in the external region, either one or two electrons can be present depending on whether excitation or ionization is being considered. The scattered electron in (3) then moves in the long-range multipole potential of $(N+1)$ electron target, which can be either in a bound or in a continuum state.

2.1.18 Optical potential methods

The Schroedinger equation describing the scattering process can be written in terms of Feshbach projection operators P and Q, where P projects onto a few target states of interest and $Q = 1 - P$. The optical potential is defined in terms of these operators by

$$V_{opt} = PVP + U, \tag{35}$$

where V is the electron-atom (atomic ion) interaction potential which is defined in terms of the total Hamiltonian by

$$H_{N+1} = K + H_N + V = H_d + V, \tag{36}$$

where K is the kinetic energy of the scattered electron and

$$U = -PH_{N+1}Q\frac{1}{Q(H_{N+1} - E)Q}QH_{N+1}P. \tag{37}$$

If we neglect U, then the resultant equations reduce to the usual close-coupling equations coupling the target states in P space. The potential U then allows for the remaining infinity of bound and continuum eigenstates and is in general both non-local and complex Both the pseudostates method and the new R-matrix method implicitly make some allowance for this potential.

$$V_{opt} = V_1 + V_2 + V_3 + \ldots\ldots\ldots\ldots, \tag{38}$$

where the first order term $V_1 = PVP$ and the second order term is

$$V_2 = PVQ\frac{1}{E - H_d + i_\varepsilon}QVP, \varepsilon \to 0^+. \tag{39}$$

In the case of elastic scattering, where P projects onto the ground state, V_1 is just the static potential and V_2 is given by

$$V_2 = \sum_{n \neq 1}\frac{<i|V|n><n|V|i>}{\frac{k_i^2}{2} - K - (w_n - w_i) + i\varepsilon}, \Sigma \to 0^+, \tag{40}$$

where we have written $H_d = K + H_n$

2.1.19. Asymptotic Green function approximation

The scattering process is complicated by three physical effects (i) the exchange of the incident electron and the target electron, (ii) distortion of the target atom charge distribution by the electric field of the incident electron and (iii) coupling between various scattering channels. The close coupling method is successfully applied to the scattering of electrons by atoms and molecules. The total wave function for $(N + 1)$ electron system consisting of an N-electron atom plus additional electron is expanded in antisymmetric products of N-electron target eigenfunctions and a set of unknown functions are calculated by solving a set of coupled integro-differential (ID) equations which are derived from the variational principle. If it were possible to retain an infinite number of terms in expansion (including the open channel) the close coupling method would yield the exact solutions to the physical problems. In practice a finite number of terms are retained. In many cases the convergence is very slow and many equations have to be solved which make the close coupling (CC) method complicated from the computational point of view. In the light of convergence problem as well as the cumbersome computational problem, Tiwary[80] has proposed an asymptotic Green function approximation (AGFA) which allows a convenient algebraic formulation of the multichannel T-matrix equation in terms of the product states of the target and the projectile. The AGFA includes all the terms of Lippmann-Schwinger (LS) equation

$$T = V + VG_0^+ \, T \tag{41}$$

with an asymptotic form of the Green function G_0^+ and the first Born approximation (FBA) corresponds to keeping only the leading term *i.e.* $T = V$ This method avoids an infinite discrete expansion of the projectile state and yields the complex scattering amplitude in a compact form. It also provides a simple way of incorporating any number of states for systematic improvement of the results. The limitation of the method depends only on the inversion of the matrix and the speed with which it can be done. For determining the excitation cross section the T matrix element is obtained in the CC method by solving a finite set of coupled ID equations by means of numerical techniques. The same matrix element is obtained in the AGFA using the LS equation and solving a finite set of the coupled algebraic equations by means of the matrix inversion technique. Both of them allow the incorporation of any number of target states in the expansion of the total wave function (electron-atom). The LS equation for the transition matrix is given by

$$T = V\,(1 - VG_0^+)^{-1}\,, \tag{42}$$

where V is the interaction potential between the target and the projectile and G_0^+ is the free particle Green function for the outgoing wave boundary condition. The T matrix, taken between the initial state i and final state f, becomes

$$< f \mid T \mid i > = < f \mid V \mid i > + \sum_j < f \mid VG_0^+ \mid j > < j \mid T \mid i >\,. \tag{43}$$

where $\mid i >$ is any given unperturbed state of the total (electron + atom) system. The Green function G_0^+ which appears in the LS equation can be written as

$$G_0^+(r, r') = -(2\pi)^{-3} \int \frac{e^{iK\,(r-r')}}{K^2 - k^2 - i\varepsilon}\, dK\,. \tag{44}$$

where the limiting process $\varepsilon \to 0^+$ is always implied. Explicitly, we have

$$G_0^+(r, r') = -\frac{1}{4\pi} \frac{e^{ik\mid r-r'\mid}}{\mid r - r' \mid} \tag{45}$$

Under the asymptotic condition, *i.e.* $r \to \infty$, the Green function becomes

$$G_0^+(r, r')_{r\to\infty} = -\frac{1}{4\pi}\frac{e^{ikr}}{r}. \tag{46}$$

with the asymptotic form of the Green function, the eq. (43) may be written as

$$< f \mid T \mid i > = < f \mid V \mid i > - \frac{1}{4\pi}\sum_j < f \quad V^{\dagger} \quad {}^{ik.r} \quad j > < j \mid T \mid i > . \tag{47}$$

2.1.20. Semi-classical impact parameter method

Many cross section calculations on system for which the concept of well defined trajectory is valid for the relative motion have been made in the impact parameter formulation. The trajectory is taken to be rectilinear, and the impact parameter b plays the role of angular momentum through the relationship

$$M\, v\, b = l\, \hbar \ . \tag{48}$$

Quantum mechanics is used to treat the electronic motion, so that impact parameter method is semiclassical. This method is most successful for high energy, heavy particle collisions and low energy transfers. An alternative approach is to integrate numerically the classical equations of motion to obtain the trajectory, or to apply classical perturbation theory to calculate it. The latter technique is applicable for large impact parameters and small energy transfers.

2.1.21 Classical trajectory Monte Carlo method

The method provides a means of evaluating collision cross section The equation governing the relative motion of the collision partners are integrated step by step on a computer for a large number of different impact parameters. The final states of the particles are determined, and the outcome of the collision is recorded. A Monte Carlo method is used for random selection of the impact parameter and the relevant target parameters (such as the position and momentum of the bound electrons). Thousands of collisions are studied, and cross sections are calculated from the relative probabilities of the various results We have here the simulation of a scattering experiment on a computer, the initial conditions for each collision being chosen by using a sequence of random physical conditions of an actual experiment

2.1.22. Classical impulse, binary encounter approximation

Here we have the classical counterpart of the quantal impulse (sudden) approximation described in the section (2.2.6). In the present case we make the following assumptions :

(a) the projectile follows a classical trajectory,

(b) initially, the target is in state i, with binding energy E_i .

The binding forces are imagined to be switched off until after the collision, when in case of excitation, for example, they are switched on again to produce a final state with binding energy E_f. This assumption is the impulse approximation.

(c) During the collision, there are no interactions among the target electrons, and the interaction of each of these electrons with the projectile may be calculated independently. The separate cross sections are summed to obtain the total cross section. The binary encounter approximation is made here.

We are assuming that the probability of a given energy transfer ΔE is the same as if the projectile were passing through a gas of free electrons whose velocity distribution is the same as that of the classical atom. Classical binary encounter theory is most approximate when the collisions are sudden (*i.e.* when the interaction time is short compared with the period of orbital motion of the target electron) and when the resulting ΔE is small.

The classical impulse, binary encounter approximation goes back to Thomson. It has been widely applied, especially to the case of the electronic and ionic projectiles impinging on neutral and ionized targets. Its success appears to be due to mainly to two factors :

(1) The correspondence principle assures us that classical theory is accurate if the action integrals associated with the interactions obey, as is the case in many types of collisions.

(2) The Coulombic potential has special properties of great importance here. For distinguishable particles interacting through it, the classical and quantal scattering formulae are identical, and for indistinguishable particles, the formulas differ only because of interference between the direct and exchange terms. Furthermore, the microcanonical velocity distribution of a target electron is the same as the quantal distribution.

2.1.23. Eikonal approximation

When the wavelength of the projectile is small compared with the distances over which the scattering potential changes appreciably, the concept of a classical trajectory acquires meaning. If r_0 is the range of the potential, the condition may be stated as

$$kr_0 >> 1 . \tag{49}$$

This condition is the basis of semiclassical scattering approximations, which have been very useful for heavy particle, and also for electron scattering. Further, if the energy of the projectile, E, is large compared with a typical value of the potential, V_0, so that

$$\frac{V_0}{E} << 1 , \tag{50}$$

the eikonal approach to scattering problems becomes feasible, as we shall show here. First let us consider the classical limit of the time independent wave equation for the projectile-target relative motion in elastic scattering by a structureless potential $V(r)$:

$$\left| -\frac{\hbar^2}{2m} \nabla^2 + V(r) - E \right| \Psi(r) = 0 \tag{51}$$

We write

$$\Psi(r) = e^{\frac{iS(r)}{\hbar}} \tag{52}$$

and obtain

$$\frac{1}{2m} \left[-i\hbar \nabla^2 S + (\nabla S)^2 \right] = E - V(r) . \tag{53}$$

We go to classical limit when $\nabla^2 S << (\nabla S)^2$, this condition being equivalent to the limit $\hbar \to 0$. In this limit, $S = S_0(r)$, and

$$\frac{1}{2m} (\nabla S_0)^2 = E - V(r). \tag{54}$$

If $S_0(r)$ is taken to be Hamilton's characteristic function, is the classical Hamilton-Jacobi equation. In optics, this equation is called the eikonal equation. By integrating, we can determine the trajectories that are normal to the surfaces $S_0(r)$ = constant. Since the normals to the surfaces are parallel to ∇S, formal solution of (54) is

$$S_0(r) = \int ds\, [2m\,[E - V(r)]]^{\frac{1}{2}}, \tag{55}$$

where the integration is along a trajectory. If we substitute S into (52) we obtain the eikonal wave function. The use of this approximate wave function in the integral equation for the scattering amplitude is the basis of the eikonal approximation. This approximation is most accurate for high impact energies or for weak interactions. It represents the relative motion of the collision partners by a distorted plane wave, and may be regarded as a first order correction to the Born approximation, which treats the relative motion as an undistorted plane wave. If the impact energy greatly exceeds the interaction energy and the internal energy of the system, the trajectory of the system will not deviate significantly from a straight line path.

2.1.24. *Multichannel eikonal treatment*

Generalization of the eikonal method to inelastic collision can be carried out by writing the system wave function as

$$\Psi(r, r_1) = \sum A_n(r)\, \psi_n(r_1) e^{\frac{iS_n(r)}{\hbar}}, \tag{56}$$

where the eikonal S_n for classical relative motion with local wave number $K_n(r)$ in channel n under the static interaction V_{nn} is the solution of

$$(\nabla S_n)^2 = 2m\,[E - E_n - V_{nn}(r)] = \hbar^2 K_n^2(r), \tag{57}$$

where E is total energy of the system and E_n is the internal energy associated with the eigenfunction Ψ_n. For a straight line trajectory for relative motion ($r = b, z$) along the Z axis, the probability amplitudes satisfy the set of coupled equations

$$\frac{i\hbar^2}{m} K_n \frac{\partial A_n}{\partial Z} = \sum_{m \neq n} A_m(b, z)\, V_{nm}(b, z)\, e^{i(S_m - S_n)}, \tag{58}$$

where b is the impact parameter. Substitution (58) yields

$$f_{in}(\theta) = \frac{1}{4\pi} \frac{2m}{\hbar^2} \sum_m < e^{iK_n z} | V_{nm}(r) | A_m(r)\, e^{iS_m(r)} > \tag{59}$$

for the scattering amplitude for $i \rightarrow n$ transitions as given by the multichannel eikonal treatment

2.1.25. *Glauber approximation*

Glauber proposed an eikonal method in which all orders of the perturbation expansion were summed, with the leading term being the Born approximation. The Glauber approximation was introduced for nuclear problems and was not applied to atomic collision until 1968. However, it has subsequently been used extensively in calculation on elastic and inelastic collisions of electrons with atoms and molecules at intermediate and high energies. One of its useful features is that it satisfies the optical theorem, thereby being applicable in certain situations where the potential is too strong for the Born approximation to be valid. Two main assumptions underlying

the Glauber approximation are (1) all important atomic states have the same energy, and (2) the scattering is confined to small angles in the forward direction. The first assumption is the closure approximation. The Glauber approximation plays an important role in focusing attention on eikonal type approximations in atomic collisions. Lately, the approximation in its original form has been seen little use as its limitations have become better understood. These limitations include (1) the nonphysical singularity in the elastic forward scattering amplitude, and (2) the alternating purely real and imaginary nature of the multiple scattering expansion.

2.1.26. Semiclassical S-matrix method

Semiclassical techniques in collision theory offer the possibility of retaining the computational simplicity of classical mechanics without sacrificing any essential quantal features. It has been applied with considerable success to elastic, inelastic, and reactive collisions between heavy particles at low energies. The development of the method began in the late 1980 and is due mainly to Miller and Marcus. Miller started from the semiclassical limit of the Feynman propagator and followed along lines similar to those that establish the eikonal relation between physical and geometrical optics. Marcus utilized the semiclassical connection between the Schroedinger and Hamilton-Jacobi equations to obtain a generalized WKB form for the multidimensional wave function. This approach is an extension of the WKB treatment of the motion in one dimension.

The semiclassical S-matrix method provides the ability to calculate accurate cross section by integrating the classical equation of motion. The scattering amplitude may be represented as an integral over all possible phase weighted classical trajectories that are relevant, with the phase expressed in terms of the classical action. The development of increasingly accurate methods of evaluating this integral has been the subject of much research. Here we have a semiclassical theory of scattering that combines exact classical dynamics with the quantal principle of superposition. All quantum effects, arising as they do from the superposition of probability amplitudes, are contained at least qualitatively within the calculations. Such effects include interference, tunneling, resonance, selection rules, diffractions, and quantization itself.

2.1.27. Methods to include relativistic effects

In previous methods, effects of exchange, polarization, channels coupling and correlation have been included but relativistic effects have been not incorporated. As the nuclear charge Ze of the target increases, relativistic effects become very important even for low energy electron scattering. There are three main ways in which relativistic effects can be introduced First, for the light weight atoms and ions where the relativistic effects are small so that the fine structure intervals between the levels of the target can be neglected in a first approximation, then the K-matrices obtained from the non-relativistic calculations can be recoupled to give cross sections between these levels. This is the basis of a program JAJOM written by Saraph[60] which has wide use in the electron-ion collisions.

Second, for intermediate weight atoms and ions, relativistic effects can be included by using the Breit-Pauli Hamiltonian

$$H^{BP}(Z, N+1) = H^{NR}(Z, N+1) + H^{REL}(Z, N+1), \tag{60}$$

where H^{NR} is the non-relativistic Hamiltonian and H^{REL} consists of one- and two-body relativistic terms resulting from the reduction of the Dirac equation and the Breit interaction to Pauli form. The Schroedinger equation with $H^{BP}(Z, N+1)$ is solved by expanding the total wave function. The conserved quantities in the collision are now JM_J and Π instead of $L\,S\,M_L$, M_S and Π. The

total angular momentum J is constructed from the total angular momentum of the target J_i through a pair coupling scheme

$$J_i + l = K,\ K + S = J, \tag{61}$$

where l, S are the orbital and spin angular momenta of the scattered electron.

Third, for heavy weight atoms and ions, relativistic effects may be taken into account by employing the Dirac Hamiltonian

$$H^D_{N+1} = \sum_{i=1}^{N+1} (c\boldsymbol{\alpha}_i \cdot \boldsymbol{p}_i + \beta_i c^2 - \frac{Z}{r_i}) + \sum_{i \neq j}^{N+1} \frac{1}{r_{ij}}, \tag{62}$$

where α and β are the usual Dirac matrices and c is the velocity of light. This approach has been implemented in a general computer program package by Norrington and Grant [111] within the R-matrix framework and Thumm and Norcross [112] have developed the Dirac R-matrix method for scattering of electrons from alkali-metal atoms and alkali-like ions.

Being rather simple one-electron like systems, alkali-metal atoms and alkali-like ions are an attractive subject for the study of their interactions with electrons. In the present review article, we have studied briefly the scattering of electrons (e) from the lithium (Li) and Li-like ions, sodium (Na) and Na-like ions, potassium (K) and K-like ions, rubidium (Rb) and Rb-like ions and cesium (Cs) and Cs-like ions.

2.2. e-Li and Li-like ions collisions

Figure 3 displays the integral cross section for the excitation of the lowest lying autoionizing level generated due to the core excitation $1s^2 2s\ ^2S \rightarrow 1s\,2s^2\,^2S$ transition in the Li atomic system by electron impact obtained employing the asymptotic Green function approximation (AGFA), R-matrix, distorted wave Born approximation with exchange (DWB^e), distorted wave Born approximation without exchange (DWB^d), Coulomb-Born approximation (CBA), and plane wave Born approximation (PWBA). It is clear from the figure that DWBA with exchange and R-matrix methods agree with each other qualitatively but differ significantly in nature from PWBA and DWBA without exchange and similar other approximations. DWB with exchange and R-matrix cross sections are still rising in the close vicinity of the threshold and decreases monotonically at high impact energies.

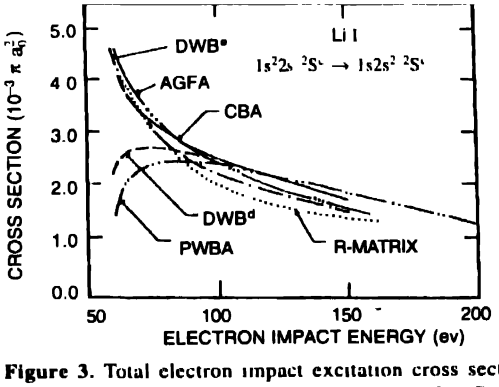

Figure 3. Total electron impact excitation cross section for the e-Li collision ——— asymptotic Green function approximation results (Ref. 82). , R-matrix results (Ref 82). –.–. distorted wave Born approximation results (Ref. 82). –..–. plane wave Born approximation results (Ref. 82). –. Coulomb-Born approximation results (Ref 82).

Figure 4 exhibits the angular distribution of electrons in the case of lithium in the DWB with exchange at different impact energies. At 70 eV, the differential cross section decreases

with the increasing scattering angle and reaches a minimum value at about 60° and then rises in the backward scattering region. It is interesting to note that the cross section in the backward direction is considerably larger than the forward direction. At 80 eV, the cross section is almost

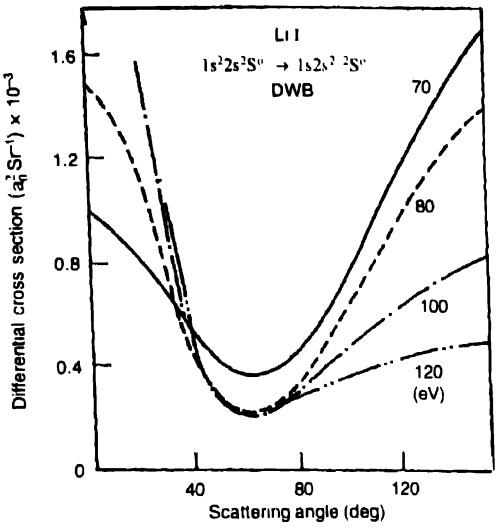

Figure 4. Differential cross section for the e-Li collision at incident energies 70, 80, 100 and 120 eV (Ref 81)

the same in the forward and backward directions. At higher energies, the forward scattering dominates over the backward which is usual behaviour. From this pattern of angular distribution as well as the abrupt rise in the integrated cross section obtained in the distorted wave Born approximation with exchange and the *R*-matrix method, it is well established that the exchange is significantly important for the resonance type character in the cross section. It also reflects that the inclusion of exchange is indispensable for obtaining accurate results. Figure 5 gives

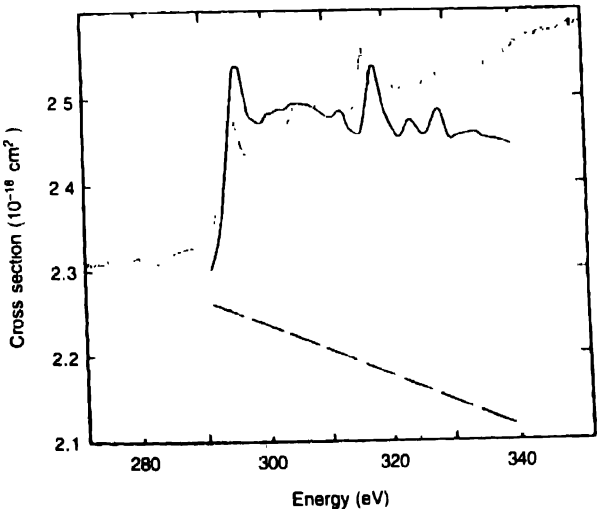

Figure 5. Electron impact ionization cross section for the ground state of C^{4+} ion of the lithium isoelectronic sequence Broken curve, direct ionization (Ref. 113, 114), full curve, direct plus EA plus REDA (Ref 115), dotted curve, experiment (Ref. 116)

the electron impact ionization cross sections for the ground state of C^{3+} ion of the lithium isoelectronic sequence. The broken curve gives the normalized direct ionization cross sections obtained by using the parameters of Younger. Full curves represent excitation – autoionization (EA) and resonant-excitation-double-autoionization (REDA) of Tayal and Henry which have been added to the direct cross section of Younger. Crossed beam experimental data of Muller *et al* are shown by the dotted curve. The increasing trend of the measured cross sections at higher electron energies is attributed by Hoffmann *et al* to uncertainty in normalization. The inner-shell excitation cross sections for the $^2S \rightarrow 1s2s2p\,^4P^0$ and $^2S \rightarrow 1s2s(^1S)2p\,^2P^0$ transitions make dominant contributions in the threshold region. The calculated features in the cross sections are in good agreement with the new crossed beam experiment. There are some discrepancies in the magnitude of the cross sections at the peaks.

2.3. e-Na and Na-like ions collisions

Figure 6 shows the low energy electron impact integrated cross section of the lowest lying autoionizing level generated due to the inner- shell excitation $1s^22s^22p^63s\,^2S \rightarrow 1s^2\,2s^2\,2p^5\,3s^2\,^2P$ transition in the Na atomic system obtained using the single configuration Hartree-Fock wave function for both the initial and final states within the R-matrix, PWBA and GA methods. There is a qualitative difference between the R-matrix and other approximations which suggests that the PWBA, GA and VPSA are not useful for the inner-shell complex excitation process.

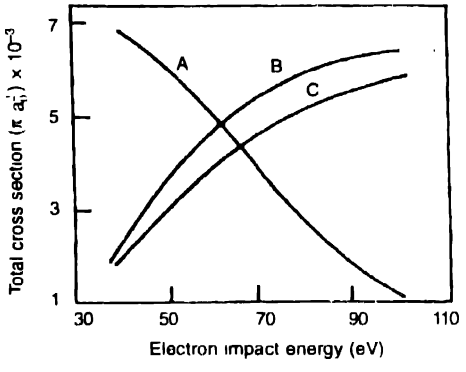

Figure 6. Total electron impact excitation cross section for the lowest lying autoionizing level in sodium. Curve A, R-matrix results (Ref 75) , Curve B, first Born approximation results (ref 75) , Curve C, Glauber approximation results (Ref 75)

Figure 7 gives the differential cross section for the elastic electron scattering on sodium atomic system obtained using coupled-channels optical (CCO) and convergent-close-coupling (CCC) methods with available theoretical and experimental data. Figure 8 displays for inelastic differential cross sections obtained using the exactly the same methods as employed in the case of the elastic scattering. The situation is encouraging. However, the discrepancy between the experiment and theory exists.

Figure 9 gives electron impact ionization cross sections for Fe^{15+} ion of the sodium isoelectronic sequence. The direct ionization cross sections calculated by Moores are given by broken curve. Indirect contributions from EA and REDA are then added successively to the direct results. The lower full curve represents total cross sections with excitation – autoionization. The upper full curve indicates total cross sections including REDA contributions as well. Both

full curves are calculated by Chen *et al.* The REDA process contributes about 30% to the average total ionization cross sections for Fe^{15+} with impact energy given in the figure. The EA cross sections are about four times the direct ionization cross sections. Experimental results of Gregory show the large fluctuations which may be associated with the REDA resonances.

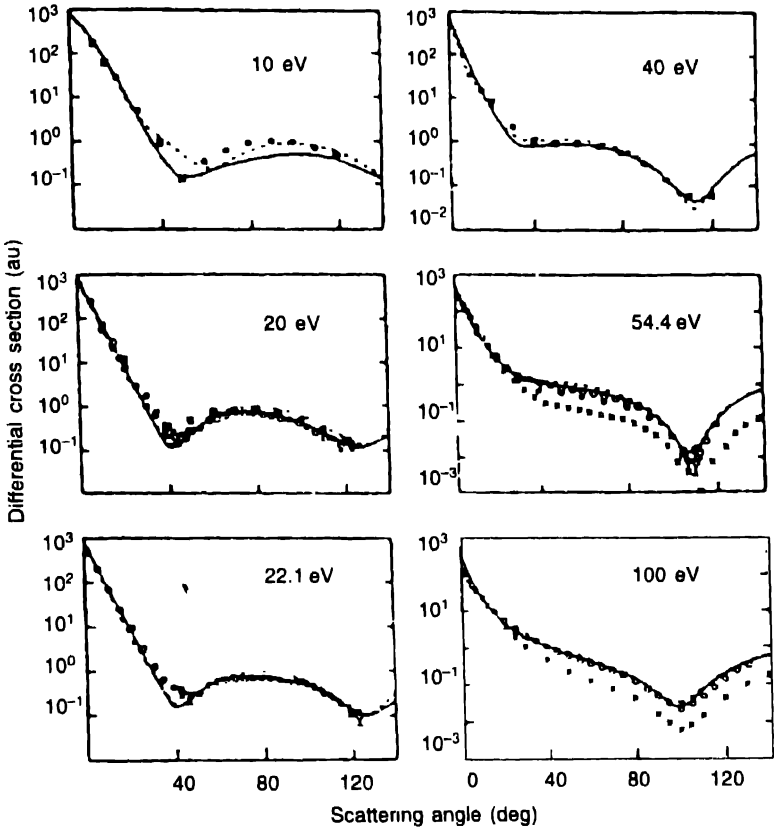

Figure 7. Differential cross section for elastic electron scattering on sodium. Open circles : Lorentz and Miller (Ref 117), closed circles : Srivastava and Vuskovic (Ref 118), crosses . 54.4 eV , Allen *et al* (Ref. 119), 100 eV , Teubner *et al* (Ref 120), solid curve : coupled channels optical (Ref 121), broken curve 3-state coupled channels (Ref. 121)

2.4 *e-K and K-like ions collisions*

Figure 10 represents the low energy electron impact integrated cross section of the lowest lying autoionizing level generated due to the inner- shell excitation $1s^22s^22p^63s^23p^64s\ ^2S \rightarrow 1s^22s^22p^63s^23p^54s^2\ ^2P$ transition in the *K* atomic system obtained using the single configuration Hartree-Fock wave function for both the initial and final states within the *R*-matrix, PWBA and GA methods. There is a qualitative difference between the R-matrix and other approximations which suggests that the PWBA, GA and VPSA are not useful for the inner-shell complex process.

Figure 11 gives the electron impact ionization cross sections for Ca^+ ion of the potassium isoelectronic sequence. The lower dotted curve represents the 4*s* subshell direct ionization

cross sections from scaled Lotz calculation. The full curve and the broken curve are the direct plus 13-state and direct plus 4-state close-coupling calculations of Badnell *et al*. The upper

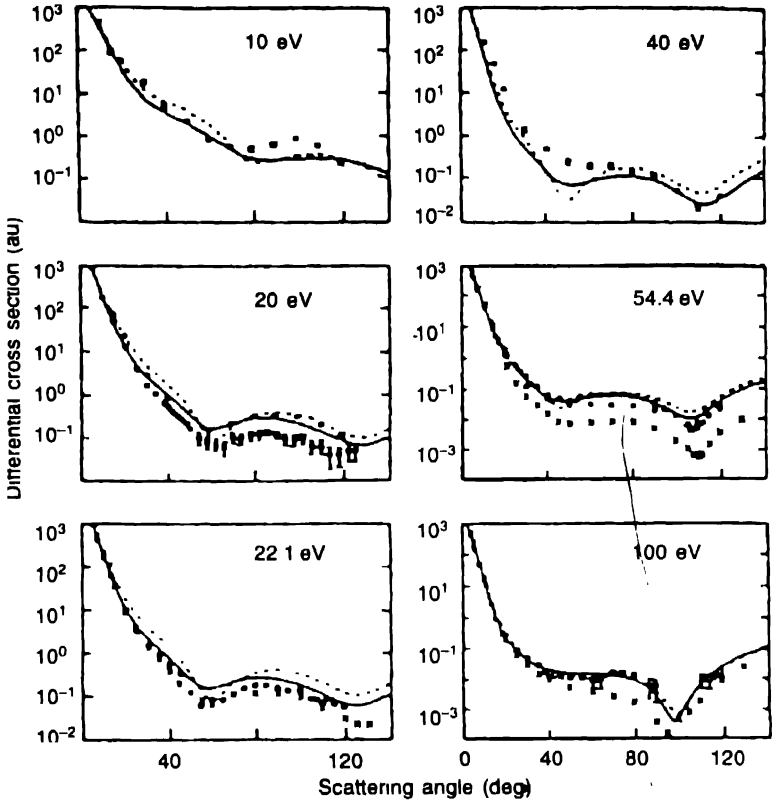

Figure 8. Differential cross section for electron scattering to the $3p$ state of sodium Open circles Lorentz and Miller (Ref 117), closed circles Srivastava and Vuskovic (Ref 118), crosses 22.1 eV ; Teubner *et al* (Ref 122), other energies ; Buckman and Teubner (Ref 123), calculations are as for Figure 7

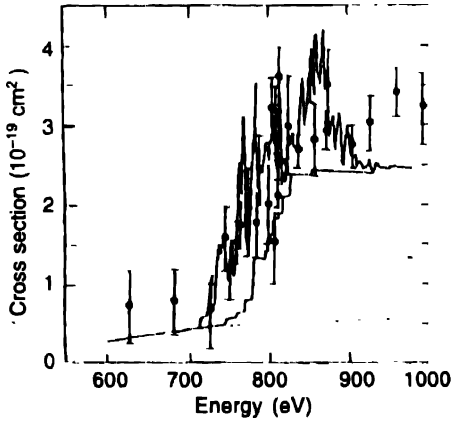

Figure 9. Electron impact ionization cross section for Fe^{14+} ion of the sodium isoelectronic sequence. Broken curve, direct ionization (Ref 124) ; lower full curve, direct plus EA (Ref 125) ; upper full curve, direct plus EA plus REDA (Ref. 125) ; full experiment (Ref. 126)

dotted curve represents experimental measurements of Peart *et al.* The latest theoretical results were obtained by multiplying each inner-shell excitation cross sections by the appropriate autoionization yield scaled to agree with experiment at the lowest energy. The four states

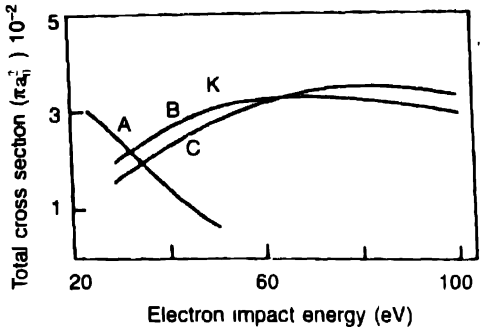

Figure 10. Total electron impact excitation cross section for the lowest lying autoionizing level in potassium
Curve A, *R*-matrix results (Ref 75) . Curve B, first Born approximation results (Ref 75) ; curve C, Glauber approximation results (Ref 75)

results are similar to those obtained previously by Burke *et al* and Pindazola *et al.* The main effect of including 13-term in the close-coupling expansion rather than 4 is to redistribute the collision strength of the resonance feature over all nine autoionizing terms.

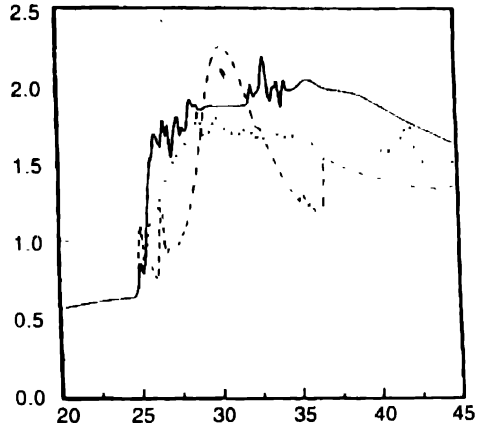

Figure 11. Electron impact ionization cross section for Ca^+ ion of the potassium isoelectronic sequence
Full curve, 13-state close-coupling calculation (Ref 127) , broken curve, 4-state close-coupling calculation (Ref 127) , convoluted with a 0.2 eV FWHM Gaussian, and added to a direct ionization cross section determined from the Lotz (Ref 128) formula, scaled to experiment ; dotted curve, experiment (Ref 129)

2.5. *e-Rb and Rb-like ions collisions*

Figure 12 represents the low energy electron impact integrated cross section of the lowest lying autoionizing level generated due to the inner-shell excitation $1s^22s^22p^63s^23p^63d^{10}4s^24p^65s \rightarrow 1s^22s^22p^63s^23p^63d^{10}4s^24p^55s^2\ ^2P$ transition in the *Rb* atomic system obtained using Vainshtein, Presnykov and Sobelman approximation (VPSA) and modified

first Born approximation (MFBA). Two features of importance emerge from the figure. Firstly, cross sections calculated in the CMA are smaller than the VPSA and MFBA. Also the maxima of the cross sections are obtained at much higher incidence energy. The second important feature is the appearance of a subsidiary maximum very close to the threshold.

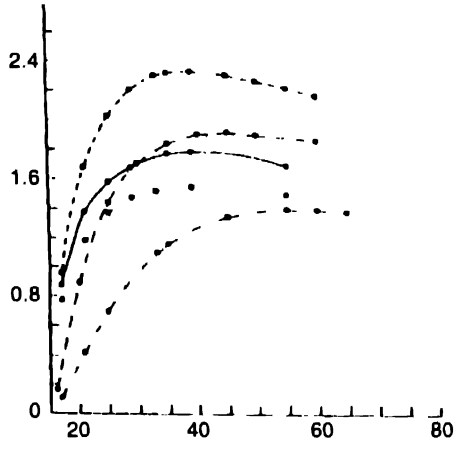

Figure 12. Integrated electron impact excitation cross section for the lowest lying autoionizing level in rubidium
Full curve, VPSA results (Ref 68), chain curve, MFBA results (Ref 68).

Figure 13 displays cross section for the ionization of Sr^+ ion of the rubidium isoelectronic sequence plotted against incident electron energy. The inset illustrates results obtained at the higher electron energies. It is clear from the figure that autoionization cross section is considerable. It also shows that a less abrupt rise in the ionization function of Sr^+ occurs between 22 and 30 eV. This is probably due to the unresolved contribution of two autoionizing states

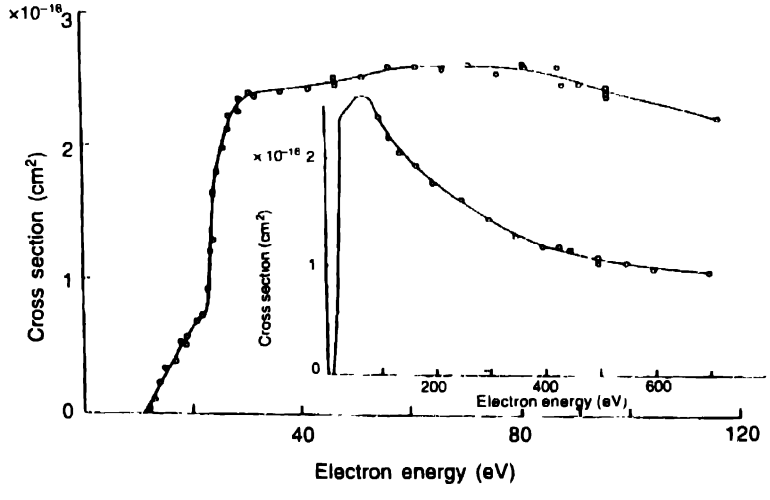

Figure 13. Cross section for the ionization of Sr^+ ion of the rubidium isoelectronic sequence plotted against incident electron energy The inset illustrates results obtained at the higher electron energies (Ref. 130).

2.6. e-Cs and Cs-like ions collisions

Figure 14 gives the low energy electron impact integrated cross section of the lowest lying autoionizing level generated due to the inner- shell excitation $1s^2 2s^2 2p^6 3s^2 3p^6 3d^{10} 4s^2 4p^6 4d^{10} 5s^2 5p^6 6s\ ^2S \rightarrow 1s^2 2s^2 2p^6 3s^2 3p^6 3d^{10} 4s^2 4p^6 4d^{10} 5s^2 5p^5 6s^2\ ^2P$ transition in the Cs atomic system obtained in the FBA, GA and AGFA in the low energy region. The FBA shows broad maximum around about 38 eV whereas the AGFA exhibits structure in the excitation function. The near threshold structure, in the AGFA curve, is more sharp and pronounced compared to the second flat maximum at nearly 38 eV. The second broad maximum appears almost in the same position where the FBA yields a maximum but the magnitude of the AGFA is smaller by a factor of about 2.5 compared to the FBA in the vicinity of maximum. The AGFA predicts a resonance like feature in the excitation function. No experimental data are available for the meaningful comparison.

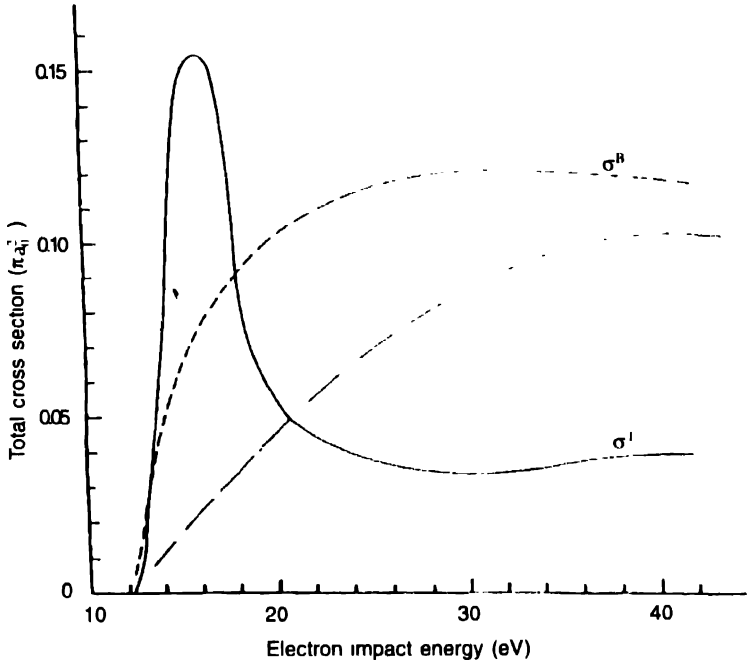

Figure 14. Total inner-shell excitation cross section (σ) for cesium as a function of electron impact energy (E)
—, asymptotic Green function approximation (Ref 79) , – – –, first Born approximation (Ref 79), –. –. Glauber approximation (Ref. 79)

Figure 15a gives the sum of the elastic and inelastic angle integrated cross sections (AICS) in the low incident energy region which is practically identical with the total cross sections for e-Cs scattering shown in the figure 15b. The most striking feature in the comparison of the Dirac *R*-matrix cross sections with other calculations is the strong $^3P^0$ resonance enhancement (Figure 15b). The non-relativistic two-state calculations predict bound $^3P^0$ state of Cs^- which explains the lack of the resonance enhancement in the scattering cross sections. The more recent semirelativistic five-state calculation shows a large discrepancy with the Dirac *R*-matrix method. The disagreement was recently traced to the inappropriate use of orbitals. The absolute measurement has an experimental uncertainty of ± 20% which is not quite enough

to overlap the Dirac R-matrix results. It is clear from the figure that there is a disagreement between the Dirac R-matrix predictions and recent experimental observations.

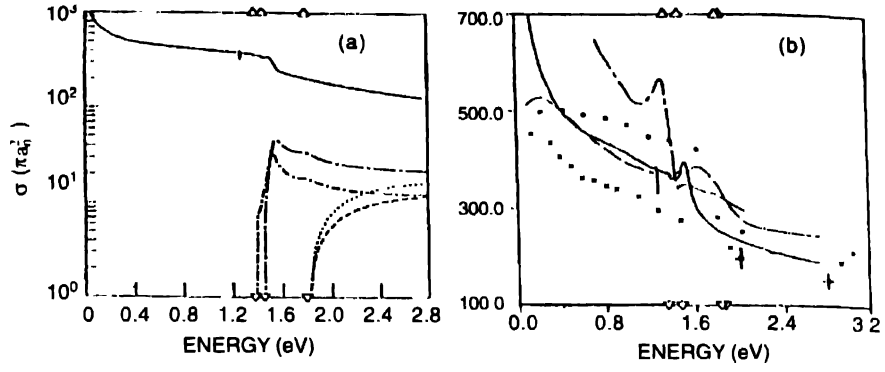

Figure 15. (a) Elastic and inelastic angle integrated Dirac R-matrix cross section for cesium and (b) Total angle integrated cross section Theory Dirac R-matrix calculation (Ref 131) (–), Ref (132) (– · · –), Ref (133) (– – –), Ref (134) (•) Experiment Ref (135) (x), Ref (136) (■). The $6P_{1/2}$ and $5D_{3/2}$ thresholds are marked by the small triangles

Figure 16 displays cross section for the electron impact ionization of Ba^+ ion of the cesium isoelectronic sequence along with the cross section of Mg^+, Ca^+ and Sr^+ ions. The figure shows that the cross section of autoionization increases with increase of atomic number (Z). It also illustrates small humps in the curves for Sr^+ and Ca^+ at energies greater than 50 and 60 eV, respectively. These are probably due to direct inner-shell ionization.

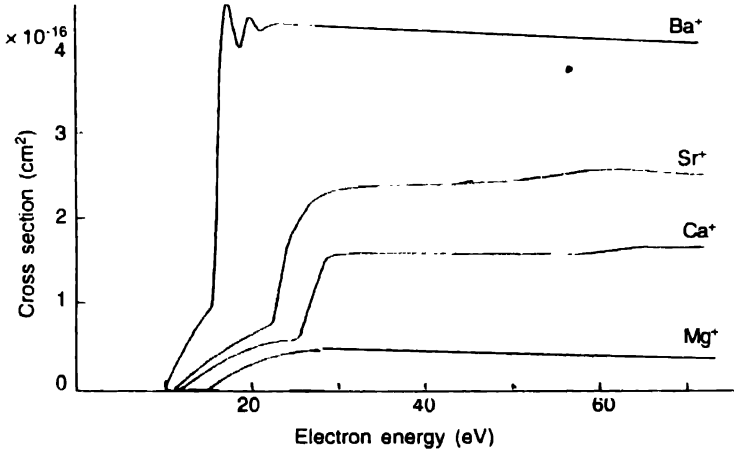

Figure 16. Cross section for the electron impact ionization of Ba^+ ion of the cesium isoelectronic sequence along with the cross section of Mg^+ ion of the sodium isoelectronic sequence, Ca^+ ion of the potassium isoelectronic sequence and Sr^+ ion of the rubidium isoelectronic sequence (Ref. 130)

3. Scattering of Photons

3.1. Review of double-continuum wave functions

The subject of various forms of double-continuum wave functions is of growing interest to theorists because it is needed to solve a very broad range of problems, for example, double-

photoionization, photo double detachment of negative ions, inner-shell photoionization followed by Auger process, electron impact single ionization, inner-shell excitation by electron impact which leads to autoionization, threshold law, *etc*. To obtain full solution of Schroedinger equation for two-electron system in any coordinate system is practically not feasible until now. Asymptotic solution is feasible. Knowledge of accurate asymptotic double-continuum wave functions is indispensable in order to perform a reliable theoretical calculation employing elaborate method. For example, *R*-matrix [63] method requires accurate functions in the outer region *i.e.* asymptotic region. Asymptotic wave functions are also used in deriving threshold law. Wannier hypothesis, which is built also in the Wannier-Rau-Peterkop (WRP) [137-139] theory, is that the probability for the double escape of two electrons is only determined by the long range interaction *i.e.* the Coulomb interaction in the zones II and III as shown below.

I	II	III
Reaction Zone	Coulomb Zone	Outer Zone

Due to this assumption only the asymptotic part of the wave function should be considered. Rosenberg [140], Rudge and Seaton [141], Rudge [142], Peterkop [143] and Burke *et al* [110] have investigated the asymptotic double-continuum wave functions. In the threshold law, the exponent of the excess energy depends only on the final state wave function *i.e.* asymptotic part of the double-continuum wave function.

Double photoionization consists in the absorption of a single photon by an atom or a molecule followed by simultaneous ejection of two electrons. The interaction of a photon with each electron is independent from the others so that double photoionization is a forbidden process unless the electronic correlation is taken into account. If two electrons with small kinetic energies leave the residual positive ion, the motion is strongly influenced and controlled by their mutual repulsion due to the Coulomb interaction $\left(\frac{1}{r_{12}}\right)$.

The interaction leads to the exchange of energy and angular momentum over long distances and therefore implies a correlation between outgoing electrons. The final state consists of an ion and two continuum electrons *i.e.*

$$\gamma + X = X^{++} + e^- + e^- . \tag{63}$$

For He atomic system, extensive investigation [144-163] of double photoionization process has been made. For *H*-system, Donahue *et al* [164] have studied in details. For H_2 system, Dujardin *et al* [165] and Le Rouzo [166] have studied the double-photoionization cross section. Threshold law for the double photoionization has also been discussed [167-187]. In the case of complex atoms and molecules, the double photoionization (DPI) process can be divided into two classes (a) the normal Auger process *via* core ionization and (b) the resonant double Auger process via resonant core excitation. From theoretical point of view, multi-electron atoms, molecules and ions are extremely difficult because of the core.

The main reasons for choosing double-continuum wave functions and double-photoionization of He, H^- and H_2 in this review are :

(1) various forms of asymptotic double-continuum wave functions are available but in the close vicinity of threshold of double photoionization [188-209], where full correlation plays an important role, accurate double continuum wave function is not obtained until now. Accurate

double-continuum wave functions have been long standing and challenging problem for theorists. Several possibilities are explored in this review.

(2) the double-photoionization has the advantage that this is dominated by electric dipole transition and the resulting final state is pure and well defined. In the case of He, H^- and H_2, the final state consists of nucleus and two outgoing electrons and hence there are no complications due to core and offers the best opportunity to test the validity of double-continuum wave function[192-214].

(3) a number of experimental observations and theoretical predictions of double photoionization cross sections [215-227] are available for two-electron systems but there is considerable discrepancy between experiment and theory which indicates that the probability for the DPI process in atoms, molecules and ions is significant because of electronic correlations. Electronic correlations have been extensively investigated by Tiwary and his co-workers[84-107].

3.1.1. Product of two plane wave functions[144]

$$\Psi(r_1, r_2) = e^{ik_1 r_1} e^{ik_2 r_2} . \tag{64}$$

3.1.2. Product of plane wave and spherical wave functions [144]

$$\Psi(r_1, r_2) = e^{ik_1 r_1} \frac{e^{ik_2 r_2}}{\cdots} . \tag{65}$$

3.1.3. Redmond wave function [140]

$$\Psi(r_1, r_2) = e^{ik_1 r_1} e^{ik_2 r_2} e^{i\gamma} . \tag{66}$$

where

$$\gamma = \frac{Z}{k_1} \ln (k_1 . r_1 + k_1 r_1) + \frac{Z}{k_2} \ln (k_2 . r_2 + k_2 r_2) + \frac{1}{k_{12}} \ln (k_{12} . r_{12} + k_{12} r_{12}) . \tag{67}$$

3.1.4. Product of two unscreened coulomb wave functions [144]

$$\Psi(r_1, r_2) = N [\phi_{\varepsilon_1}(r_1) \phi_{\varepsilon_2}(r_2) + \phi_{\varepsilon_1}(r_2) \phi_{\varepsilon_2}(r_1)] , \tag{68}$$

where

$$\phi_\varepsilon(r) = N' F_l\left(\frac{\eta_e}{k_e}, r\right) y_{lm}(\hat{r}) , \tag{69}$$

$$F_l(k, r) \approx (2kr)^l e^{ikr} {}_1F_1(\tfrac{1}{k} + l + 1, 2l + 2, -i2kr) . \tag{70}$$

3.1.5. Brauner et al wave function [214]

$$\Psi(r_1, r_2) = e^{ik_1 r_1} {}_1F_1\left(\frac{i}{k_1}, 1, i(k_1 . r_1 + k_1 r_1)\right.$$

$$\cdot e^{i(k_2 \cdot r_2)}\, {}_1F_1\left(\frac{i}{k_2}, 1, i(k_2 \cdot r_2 + k_2 r_2)\right)$$

$$\cdot e^{i(k_{12} \cdot r_{12})}\, {}_1F_1\left(\frac{i}{k_{12}}, 1, i(k_{12} \cdot r_{12} + k_{12} r_{12})\right) \tag{71}$$

3.1.6. Altick monopole wave function [210]

$$\Psi = \rho_1^{\frac{i}{k_1}} e^{ik_1\rho_1} \rho_2^{\frac{i\varsigma}{k_2}} e^{ik_2\rho_2} + \rho_2^{\frac{i}{k_1}} e^{ik_1\rho_2} \rho_1^{\frac{i\varsigma}{k_2}} e^{ik_2\rho_1}$$

$$\cdot \left[(\rho_1\rho_2)^{-\varsigma_1} \left(1 - \frac{\varsigma_1\rho_1}{\varsigma_2\rho_2} / 1 - \frac{\varsigma_1}{\varsigma_2}\right)^{\varsigma_1 - \varsigma_2}\right]. \tag{72}$$

3.1.7. Altick dipole wave function [211]

$$\Psi = \rho_1^{\frac{i}{k_1}} e^{ik_1\rho_1} \rho_2^{\frac{i\varsigma}{k_2}} e^{ik_2\rho_2} f_{l_1 l_2}(y) \cdot \rho_2^{\frac{i}{k_1}} e^{ik_1\rho_2} \rho_1^{\frac{i\varsigma}{k_2}} e^{ik_2\rho_1}$$

$$\cdot \left[(\rho_1\rho_2)^{-\varsigma_1} \left(1 - \frac{\varsigma_1\rho_1}{\varsigma_2\rho_2} / 1 - \frac{\varsigma_1}{\varsigma_2}\right)^{\varsigma_1 - \varsigma_2}\right] g_{l_1 l_2}(y). \tag{73}$$

3.1.8. Peterkop wave function [143]

$$\psi = A(\Omega)\, R^{-n_0} e^{iS_f + i\gamma}, \tag{74}$$

where Ω = a set of five angular variables

and

$$\gamma = \omega(\Omega) \ln R + \beta(\Omega), \tag{75}$$

$$R = \sqrt{(r_1^2 + r_2^2)}. \tag{76}$$

3.1.9. Rau wave function [138]

$$\Psi_{\varepsilon \to 0} = \chi(R)\, e^{iCR^2 \left(1 + a\beta^2 + \frac{b}{ic}\gamma^2\right)}, \tag{77}$$

where

$$\chi(R) = R^{-(a+b+9/4)}, \tag{78}$$

$$a = (-1 + 2\mu)/8,$$

$$b = (-1 + i2\rho)/4,$$

$$c = \sqrt{8z_0}, \tag{79}$$

$$\mu = \frac{1}{2}((100z-9)/(4z-1))^{\frac{1}{2}}, \tag{80}$$

$$\rho = \frac{1}{2}((9-4z)/(4z-1))\frac{1}{2}. \tag{81}$$

3.1.10. Rudge-Seaton wave functions [141]

$$\Psi_{\varepsilon\to 0} \approx BR^{(n-\frac{5}{2})}e^{iAR^{\frac{1}{2}}} \tag{82}$$

$$\Psi_{\varepsilon\neq 0} \approx (-i)^{\frac{1}{2}}\left(\frac{k^3}{R^5}\right)^{\frac{1}{2}} f(kr_1 \sin(\alpha), kr_2 \cos(\alpha)) \, e^{i((kR+\zeta(r_1 r_2,\alpha))/k}\ln(2kR), \tag{83}$$

$$d = \arctan(r_2/r_1). \tag{84}$$

3.1.11. Burke et al wave function [110]

In the new R-matrix theory, two continuum electrons are expanded in terms of a continuum R-matrix basis. In addition, a two dimensional R-matrix propagator approach is developed that enables the internal region to be subdivided and highly excited target states that extend out to large distances to be treated. Analytical form of this double continuum wave function as well as application of this function to double photoionization process are not available in the literature.

3.1.12. Double-continuum wave functions in the entire space

Asymptotic wave functions are not adequate at small distances. One needs wave functions which are valid in the entire configuration space *i.e.* double-continuum wave functions which can be obtained solving the Schroedinger equation for two-electron systems without imposing any constraints but unfortunately this is not feasible. For this reason, we will describe several possible models which are valid in different physical situations.

Models without correlations : Independent particle

At very high incident energies, two ejected electrons are very far away from the residual ion, one can argue that two escaping electrons do not experience Coulomb force. Under this situation, one can describe two electrons by a product of two plane waves. Product of two plane waves gives the threshold law which differs completely from the experimental threshold law. No matter, how far or how fast electrons are, they always experience Coulomb force. Hence, this model is the crudest model and is used in the first Born approximation. Since, electrons always experience Coulomb force, so widely used model is product of two Coulomb wave functions. This model has been used in the calculation of double photoionization cross section of helium and hydrogen molecule. Since, this model does not contain correlation, hence it gives linear threshold law which disagrees with experiment. Another possible physical situation may occur at intermediate energy range that one electron is slow and another fast. The slower electron

may screen the fast one. In this case, one electron can be described by Coulomb wave function and faster one can be described by plane wave. This model also gives the threshold law which disagrees with the experiment. For reliable calculations of double photoionization cross section, one needs correlated double-continuum wave function especially in the vicinity of the threshold where electron correlations play an extremely important role in order to obtain accurate results. Such wave functions are not available in the literature.

Recently, Burke *et al* [110] have developed a new R-matrix formulation to handle double-continuum wave functions but there is no any results available until now. Other possibilities, which are feasible in the near future, are combination of the standard R-matrix with (1) Altick asymptotic wave function, (2) hyperspherical function, (3) screened Coulomb function and (4) distorted wave function with dynamic screening.

3.2. Threshold laws

There has been interest in the extensive theoretical and experimental investigations of threshold laws for escape processes, for example, double photoionization, electron impact ionization, etc in atoms, molecules and ions because these laws provide answers of many fundamental questions in physics. A number of theoretical and experimental studies of these laws have been made for different escape processes. As we have mentioned earlier in this review, our main emphasis will be to study double photoionization threshold law in atoms, ions and molecules *i.e*

$$h\nu + X \rightarrow X^{++} + e^- + e^-, \tag{85}$$

where X stands for atom or molecule or ion

This requires a solution of three charged particles with Coulomb forces acting between them. The final state of reaction consists of $X^{++} + e^- + e^-$ where there are two attractive Coulomb forces, each electron being attracted by residual ion X^{++} and one Coulomb repulsive force, electron-electron interaction $\frac{1}{r_{12}}$. If we ignore the repulsive force, the quadratic dependence on E would be reduced to a linear dependence of E. If the double-continuum electrons are represented by a product of two Coulomb wave functions, one can expect a linear threshold law because only two attractive Coulomb forces have been taken into account. Complication arises when three charged particles with Coulomb interaction are considered because of the electron correlation. To represent the final two-electron into the continuum as a product of single particle functions is only an approximation and even then there are different choices. For example, one could argue that in the neighbourhood of the threshold, as two electrons escape, there is some discrepancy in how the energy in partitioned between them, so that the slower one sees the full Coulomb field of the residual ion but the faster sees a completely screened and therefore neutral field. In this case, the final state is a product of a Coulomb wave function and a plane wave function and then there is

$$\sigma^{2+} \propto \varepsilon^{3/2} \tag{86}$$

Different assumptions on the relative screening in the escape process lead to different threshold laws. A successful threshold theory provides information on the mutual dynamic screening and mutual Coulomb repulsive interaction.

The double photoionization threshold law is

$$\sigma^{2+} \propto \varepsilon^{\beta} \tag{87}$$

where $\varepsilon = \varepsilon_1 + \varepsilon_2$ = excess energy available to two-coutinuum electrons,

$= (E_\gamma - I^{2+})$ if the residual ion is in the ground state,

E_γ = incident photon energy,

I^{2+} = double ionization threshold,

and β = exponent = 1.056

or

$$\sigma^{2+} = \sigma_0 \varepsilon^\beta , \tag{88}$$

where σ_0 is the constant of proportionality and $\sigma_0 = \sigma^{2+}$ at $\varepsilon = 1$ eV,

where exponent β depends only on the final state wave function *i.e.* the double-continuum wave function. It reflects that accuracy of double-continuum wave function can be tested by calculating the exponent *i.e.* β offers the best opportunity to test the accuracy of the final state wave function. The question is how the accuracy of the initial state wave function plays an important role in obtaining reliable double photoionization cross section. One can argue that σ_0 depends on the accuracy of the ground state wave function. Another question, immediately arises that does σ_0 depend on only the initial state or both initial and final states wave functions? There are many questions which one can ask. Byron and Joachain [144] have calculated the double photoionization cross sections using the correlated wave function for the ground state and uncorrelated wave function for the final state. Their results are not in agreement with the recent experiment which indicates that the correlation in the final state is necessary. Le Rouzo has performed similar calculation for the DPICS of hydrogen molecule.

His result is in good agreement with the experimental data of Dujardin *et al.* He has obtained the linear threshold law and is valid up to about 10 eV above the threshold. Tiwary [154-158] has performed calculation of DPICS of He using correlated initial state wave function and partially correlated final state wave function and obtained in good agreement with experimental data in the intermediate and high energy range and in the vicinity of the threshold the situation is unsatisfactory. This may be due to the lack of full correlation in the final state wave function because the correlation is extremely important in the neighbourhood of the threshold. Carter and Kelly [159] have calculated the DPICS of He using the many-body perturbation theory (MBPT). They have obtained good agreement with the experiment. Since their approach is non-wave function approach it is difficult to draw any definite conclusion

Experimental Test of WRP

Threshold Law of Double-photoionization of He

Very recently, Kossmann *et al* have performed an extensive experimental investigation of the threshold law for the cross section of double photoionization of He. Figure 19a represents experimental results of Kossmann *et al* for the threshold cross section of double photoionization of He from threshold to 83 eV photon energy. Figure 19b exhibits the same data but smaller and enlarged energy scale. The solid line in both figures represents in a limited energy range a least square fit of the experimental data by the power law. Because of the small difference between a linear threshold law ($\beta = 1$) and the expected $\beta = 1.056$ non-linear threshold law, it appears from the Figure 19 that linear threshold law is valid for the double photoionization of He. Quantitative analysis of results clearly show the WRP threshold law is valid because theoretical $\beta = 1.056$ and experimental $\beta = 1.05 + 0.002$ clearly demonstrates that it is indispensable to include full

correlations in both initial as well as final states involved in the transition in order to obtain reliable results.

3.3. Double-photoionization of He ($^1S^e$)

Double photoionization of noble gas atoms has been of great interest to both experimentalists as well as theorists because double-electron photoionization in noble gases gives fundamental information on the electronic correlation. Helium, which is the simplest noble gas atom is more interesting because there is no complications due to core in the double photoionization process. A number of experiments and calculations have been carried out for the DPI of He. Figure 17 displays all available experimental as well as theoretical ratio of double to single photoionization cross sections. For the first time, Byron and Joachain [144] performed calculation for the DPI of He using uncorrelated wave functions for both ground as well as the final states and correlated wave function for the ground state and uncorrelated product of two Coulomb wave functions with effective charge 2 for both outgoing electrons for the final state (reaction is shown below).

$$h\nu + He \rightarrow He^{++} + e^- + e^- \tag{89}$$

Results of DPI of He with uncorrelated wave functions for both initial and final states involved in the transition amplitude are extremely small which indicate that the probability of DPI process is very poor without correlations. Results with almost fully correlated wave function for the ground state and uncorrelated wave function for the final state are in excellent agreement with the first experiment of Carlson (see Figure 17). Agreement suggests that the correlation is important in the initial state, not in the final state. The recent experimental observations of Holland *et al* [146] disagree considerably throughout the energy range of consideration with the experimental data of Carlson [145] and theoretical prediction of Byron and Joachain [144]. This experimental result suggests that correlation, probably, is equally important in both initial and final states involved in the transition. Results of Holland *et al* are in accord with the

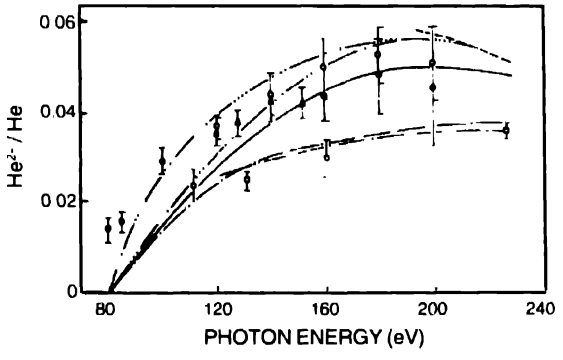

Figure 17. The ratio of cross sections He^{++} / He^+
Experimental curves
●, Holland *et al* ▲, Wight and Van der Wiel ○, Schmidt *et al* □, Carlson
Theoretical curves
---, Tiwary obtained from momentum matrix elements
– –, Tiwary obtained from position matrix elements
– —, Byron and Joachain with almost full correlation in the ground state
– – – –, Byron and Joachain with no correlation in both initial and final states
– – –, Brown · · ·, Amusia *et al* – Carter and Kelly

experimental points of Schmidt *et al* at low energies and tend to lie lower than the curve of Wight and Van der Wiel [148].

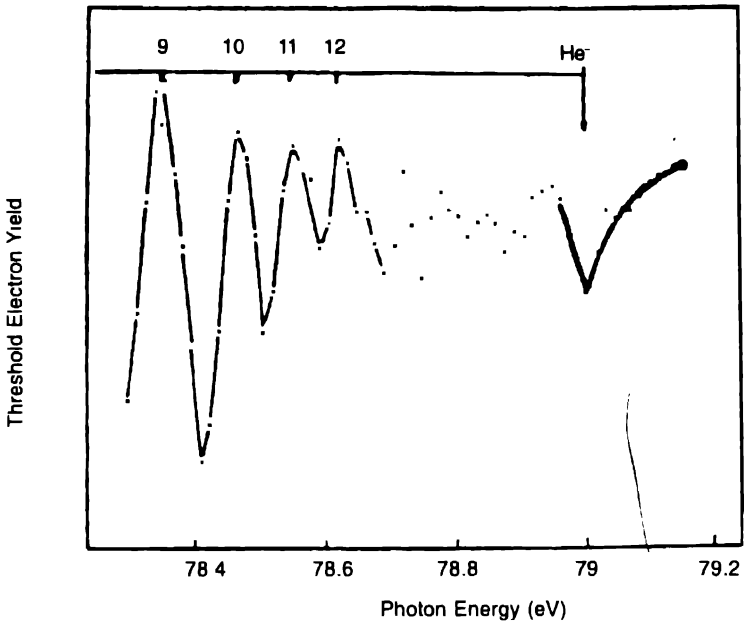

Figure 18. Yield of very low energy electrons following photon impact on He

Brown [149] has reevaluated the DPI cross section of He using a Hylleraas type wave function without decomposition into partial waves and Coulomb function for the final state His results favour the oldest experimental data and the theoretical results of Byron and Joachain Amusia *et al* [150] have also investigated this problem in the limit of high, non-relativistic photon energies. Their method leads to a greatly overestimated cross section in the energy range of recent measurements. Yurev [152] and Varnavshikh and Labzovskii [153] have performed the calculations for the DPI cross section of He in the threshold energy region using perturbation

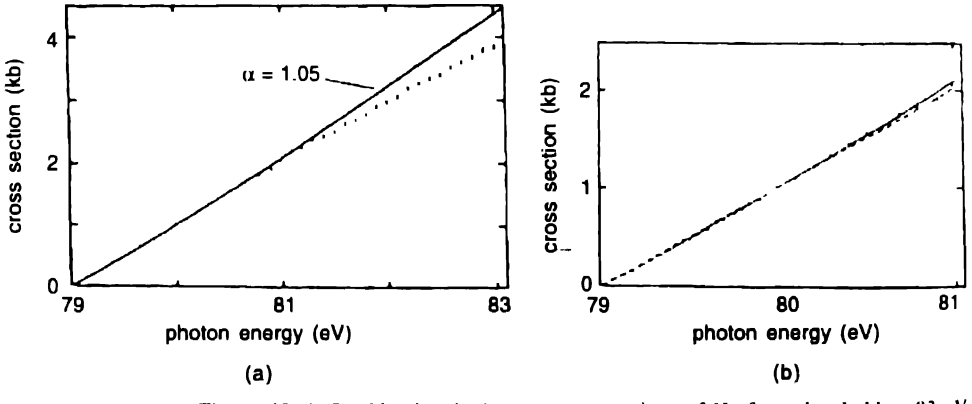

Figure 19(a). Double-photoionization cross sections of He from threshold to 83 eV photon energy
..... Experimental data of Kossmann *et al* — . Least squire fit.
(b). Same as in Figure 19(a) with smaller and enlarged energy scale.

and variational methods respectively. Their results are in qualitative agreement with each other, but are limited to the low-energy range (not shown in the figure). Tiwary [154] has performed calculations for the DPI cross section of He using the position and momentum dipole matrix elements. Tiwary has employed almost fully correlated wave function for the ground state and partially correlated wave function of Altick for the final state to evaluate dipole matrix elements. The values obtained from the length formulation tend to lie higher than those obtained using the velocity formulation. Both differ considerably from the first experimental observations and first theoretical predictions and tend to lie close to the recent reliable experimental curve of Holland *et al* [146] especially in the high energy range. There is considerable discrepancy between theoretical results of Tiwary and experimental data of Holland *et al* in the vicinity of the threshold. This clearly indicates that (1) inclusion of correlation in the final state is important, (2) partial correlation is not adequate to obtain accurate results in the vicinity of the threshold *i.e.* two outgoing electrons are very slow. The effect of correlation decreases with increase of incident photon energy. It seems to be plausible because when escaping electrons are slow, they have enough time to develop correlations. Carter and Kelly [159] have performed calculation for the DPI cross section of He using the many-body theory (MBPT) incorporating full correlation in both initial and final states. Their results are in good agreement in the entire energy range with the most recent and reliable experimental data of Holland *et al*.

3.4. Double-photoionization of H⁻ (^1S)

Double photoionization of H^- negative ion by single photon impact has been measured by Donahue *et al* [164] using a crossed-relativistic beam technique with sufficient energy resolution and close enough to threshold to yield an exponent of excess energy in the threshold law. Intercepting them with laser photons Doppler shifts the photon energy in the frame of the ion to energies greater than 14.35 eV require for double detachment.

$$h\nu + H^-(^1S) \rightarrow H^+ + e^- + e^- \tag{90}$$

The threshold cross section data are shown in the Figure 20.

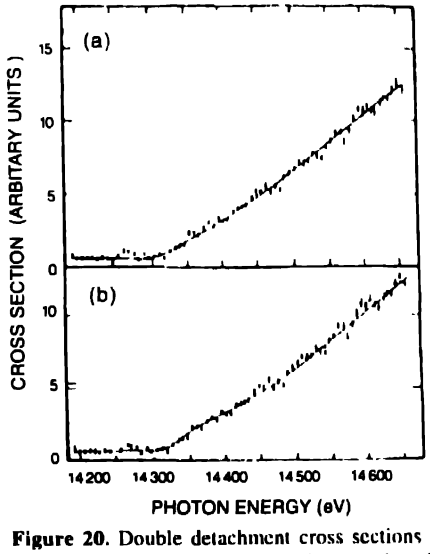

Figure 20. Double detachment cross sections for H
– –, Experiment of Donahue *et al* —, best fit by power and law and modulated linear law in Figures 20(a) and 20(b) respectively.

The data can be fitted quite accurately to the form

$$\sigma(E) = A(E - E_t)^m + B \tag{91}$$

The fit results are

$$A = 38.5 + 1.5$$

$$B = 0.68 + 0.05 \tag{92}$$

Although Donahue *et al* noted that they can also fit to an alternative result such as

$$\sigma(E) = A(E - E_t)(A + DSin(C \ln(E - E_t) + F)) + B \tag{93}$$

The results of the fit are given in details by Donahue *et al.*

The experimental arrangement suffers, unfortunately, from a spurious two electron signal which sets in at energies slightly lower than 14.35 eV. This uncertainty in the threshold position, coupled with undetermined parameters prevents an unambiguous discrimination between the two results. Laboratory experiments on double detachment of negative ions can overcome some of these problems but results of sufficient accuracy in the close vicinity of the threshold are still unavailable.

3.5. *Double-photoionization of* H_2 ($^1\sum_g^+$)

It is interesting to both experimentalists as well as theorists to extend the studies of the double photoionization of helium atomic system to another system with only two electrons with molecular symmetry, *i.e.*, hydrogen molecule, although molecular hydrogen will be more complicated because of more degrees of freedom *i.e.* vibrations and rotations. For the first time, Dujardin *et al* [165] have measured the cross section of double photoionization of hydrogen molecule by single photon impact

$$h\nu + H_2 \rightarrow H^+ + H^+ + e^- + e^- \tag{94}$$

using the photoion-photoion coincidence (PIPICO) method in the energy range 47.5 eV to 140 eV. Le Rouzo treated this problem exactly in the same way as Byron and Joachain treated the

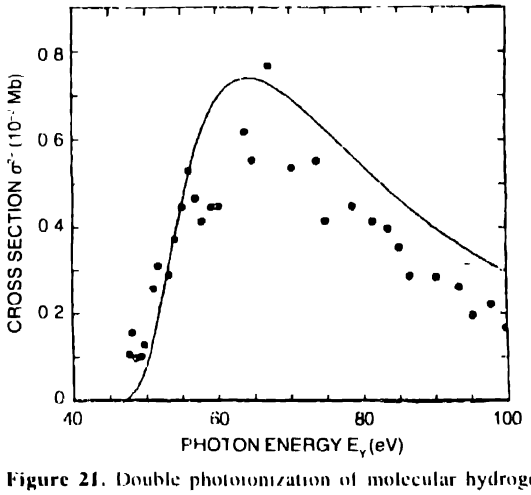

Figure 21. Double photoionization of molecular hydrogen
Experiment of Dujardin *et al* — , *R*-averaged theoretical results of Le Rouzo

double-photoionization (DPI) of helium atomic system. Le Rouzo [166] performed calculation for the DPI of hydrogen molecule in the length and velocity forms using almost fully correlated wave function for the ground state and product of two unscreened Coulomb wave functions for the final state. Figure 21 displays the experimental observations of Dujardin *et al* and theoretical prediction of Le Rouzo. It is seen from the figure that there is an excellent agreement between experiment and theory. Figure 22 displays the double photo-ionization of molecular hydrogen in the threshold region. Figure 23 exhibits comparision of the cross sections derived from the molecular threshold law (dashed curve) with the R-averaged one (solid curve) over the whole photon energy range.

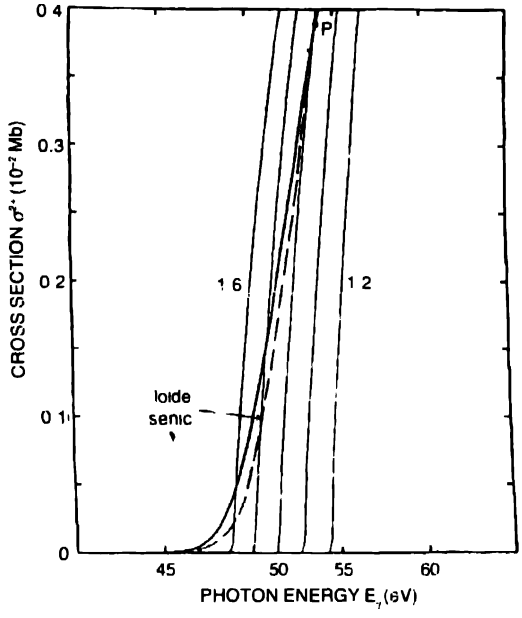

Figure 22. Double photoionization of molecular hydrogen in the threshold region – – –, Molecular threshold law matched onto the exact theoretical result at point P

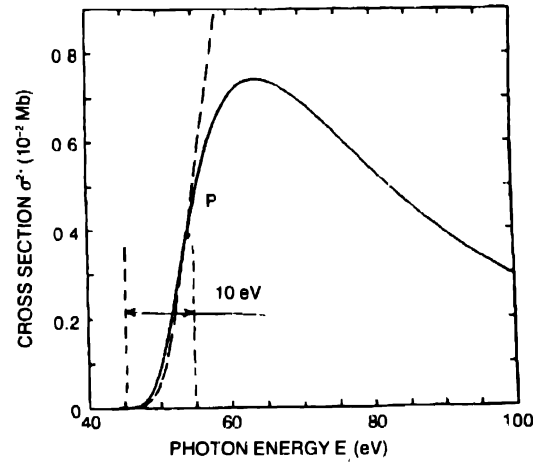

Figure 23. Comparison of the cross sections derived from the molecular threshold law (dashed curve) with the R-averaged one (solid curve) over the whole photon energy range

This suggests that it would be interesting to perform more refined experiments and calculations with full correlations in both the initial as well as final states involved in the transition. It would also be interesting to see the effect of two-centre wave function for the final state in the case of hydrogen molecule. It is well known that the exponent of excess energy depends only on the asymptotic part of the final state wave function and molecular threshold law modified due to vibrations. The product of two unscreened Coulomb wave functions gives linear threshold law and hence the result of Le Rouzo obeys the linear threshold law which disagrees with experiment.

Threshold triple differential cross section of double-photoionization of two-electron systems :

The threshold triple differential cross section (TDCS) for the double-photoionization (DPI) of two-electron systems by impact of light is very sensitive to the electron-electron correlations. Most recently, Pont *et al* [204] have applied two different methods to the calculation of TDCS for double-photoionization of helium. In one method, the 3C method, the final state is described by a product of 3 Coulomb continuum wave functions, while in the other method, the 2SC method, the final state is described by a product of 2 screened Coulomb wave functions employing effective charge

Figures 24 and 25 show the theoretical results of Pont *et al* along with the data of Lablanquie *et al* [186], for both (a) equal and (b) and (c) unequal energy sharing. The different plots have been rescaled so that the TDCS has the same value at its maximum for all sets of data in a given case. The agreement between the (rescaled) results of the 2SC calculation and the length-gauge version of the 3C calculation is good in all cases apart from the two unequal - energy sharing cases at higher excess energy. Finally, it is seen that the qualitative agreement

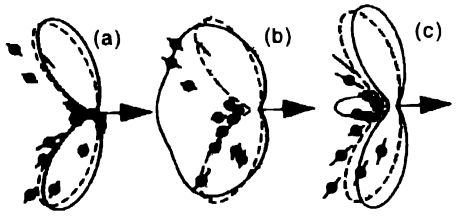

Figure 24. Polar plots of coplanar TDCS
Electron 1 emerges along the polarization axis (see arrow), and E = 4 0 eV, with (a) E1 = E2 = 2 0 eV , (b) E1 = 3 3 eV, E2 = 0 7 eV , and (c) E1 = 0 7 eV, E2 = 3.3 eV Experimental data are from Ref (186) Solid and dashed lines are from velocity and length gauge version of 3C theory, respectively, and the plotted line is from 2SC theory Plots have been rescaled so that TDCS has same value at its maximum

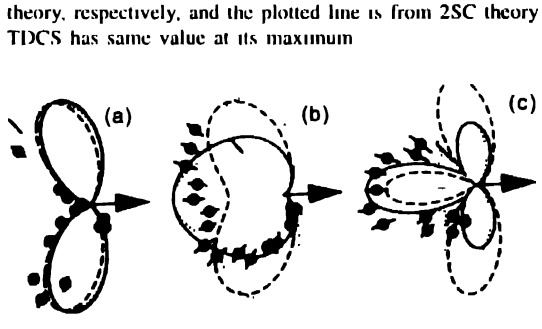

Figure 25. Same as in Figure 24 but with E = 18 6 eV and (a) E1 = E2 = 9 3 eV ; (b) E1 = 15 6 eV, E2 = 3.0 eV ; and (c) E1 = 3.0 eV, E2 = 15.6 eV

between the results of the 2SC calculation and experimental data is rather poor, the 2SC results lie, for the most part, well outside the error bars of the experiment.

4. Conclusions and future directions

The discussion of the preceding sections demonstrates that the new R-matrix, coupled-channels optical potential (CCOP) and close-coupling with the pseudostates basis functions (CCPSBF) methods, which provide a way to incorporate the effects of coupling of the target states to the continuum, have produced very accurate results for the scattering cross sections. Accurate collision cross section also depends on the structure of the target. Consequently, the exact evaluation of the cross section is possible only if the exact scattering theory as well as structure theory are employed in the calculations. It is seen that the discrepancy exists between the high precision experimental observation and high precision theoretical prediction which indicates that at present we do not have a comprehensive and practical method for the scattering and structure which is capable of yielding exact results.

A hybrid theory, which combines the effectiveness of the new R-matrix method with CCOP and CCPSBF methods, may provide the best hope for a unified theory which may be capable of producing excellent results. With rapidly increasing computer power, it is most probable that the future development may take place more and more recourse to numerical methods. It is possible that several theoretical models outline in the present review article may eventually be superseded by powerful and accurate numerical algorithms. Nevertheless, we believe the need of these methods described in this article to understand some physics of electron-atom scattering processes will remain for ever.

Great experimental and theoretical advancement has been made in the case of double photoionization (DPI) of two-electron systems but there is considerable discrepancy in the close vicinity of the threshold where correlations play an extremely important role. To obtain accurate double-continuum wave function in the vicinity of threshold is still challenging problem for the theorists. Kossmann *et al* have measured the slope (σ_1) for the DPI of He but there is no theory to evaluate the slope directly. Dynamic screening *i e.* energy dependent screening is crucial especially when two slow electrons are escaping the positive ion but there is no method available to include the dynamic screening in the Coulomb wave function, Altick wave function, distorted wave function or any other wave functions. Unscreened Coulomb wave functions gives linear threshold law which disagrees with experiment. This suggests that a method should be developed to incorporate dynamic screening. In the case of even the simplest H_2, the DPI process has not been extensively investigated either experimentally or theoretically. There is one experimental result and one theoretical calculation with Coulomb wave function. Agreement is excellent between experiment and theory but this may be fictitious. The agreement reflects that the DPI of H_2 should be reinvestigated. In the case of He, many body perturbation theory, which includes full correlations in both initial and final states, yields results which are in good agreement with the recent experiment. It clearly indicates that it is indispensable to incorporate full correlation of equal amount in both states involved in the transition in order to obtain reliable results. Angular distribution and energy sharing of two escaping electrons have not been studied but these can offer the opportunity to test the validity of a theoretical model as the exponent of excess energy does in the threshold law.

It is clear that there are numerous difficulties in obtaining the accurate double-continuum wave functions which play an extremely important role in reliable double-photoionization cross

sections. However, we would like to make some constructive and fruitful suggestions for obtaining correlated double-continuum wave functions which may be the future directions :

(1) a new R-matrix developed by Burke *et al* [110] may be very useful for the double-continuum wave function (DCWF),

(2) the standard R-matrix [63] may be combined with the Altick asymptotic DCWF and hyperspherical DCWF,

(3) solving the Schroedinger equation including the higher terms of the Neumann series,

(4) developing some new ideas and techniques which provide to include the dynamic screening in the Coulomb, Altick and distorted wave functions and finally

(5) developing some sophisticated numerical procedure to describe two continuum electrons in the entire configuration space.

In short, our knowledge of high-precision scattering, structure of atoms and atomic ions where relativity and quantum electrodynamic play an important role, double-continuum wave function as well as double-photoionization cross section of atoms, molecules and ions, particularly for heavy atoms, molecules and ions, is by no means complete. Comprehensive and painstaking work needs to be done and the field will continue to grow, develop and flourish. The future holds many challenges for both experiment and theory.

Acknowledgments

The author would like to thank the International Centre for Theoretical Physics, Trieste, Italy and Indian Institute of Science, Bangalore, for hospitality and Swedish Agency for Research Cooperation with Developing Countries (SAREC) for financing my visit. He is grateful to Prof. S. C. Mukherjee and Prof. Ter-Kazarian for encouragement and discussion.

References

[1] W C Roentgen *Sitzungsber Wuerzburger Physik-Medic Gesellsch* (1895) (Reprint, *Ann Phys Chem* **64** 1 (1898))

[2] J Franck and G Hertz *Phys Ges Verhandlugen* **D 16** 512 (1914)

[3] M Born *Z Physik* **38** 803 (1926)

[4] J R Oppenheimer *Phys Rev* **32** 361 (1928)

[5] C Ramsauer *Ann Phys* (Leipig) **66** 546 (1921)

[6] C Ramsauer and R Kollath *Ann Phys* **3** 536 (1929)

[7] A L Hughes and V Rojansky *Phys Rev* **34** 284 (1929)

[8] H C Brinkman and H A Kramers *Proc Acad Sci* Amsterdam **33** 973 (1930)

[9] H A Bethe *Ann Phys (Leipig)* **5** 325 (1930)

[10] C Ramsauer and R Kollath *Ann Phys* **12** 529 (1932)

[11] H S W Massey and R A Smith *Proc Roy Soc* (London) **142** 142 (1933)

[12] H S W Massey and C B O Mohr *Proc Roy Soc.* (London) **A 144** 188 (1934)

[13] H S W Massey and E H S Burhop *Electronic and Ionic Impact Phenomena* (Oxford Clarendon) (1952)

[14] L D Landau and E M Lifshitz *Quantum Mechanics, Non-Relativistic Theory*, 2nd edn (Reading, Mass Addison-Wesley) (1965)

[15] A Messiah, *Quantum Mechanics* (New York : Interscience) **Vol. I** (1961), **Vol. II** (1962)

[16] E Merzbacher *Quantum Mechanics*, 2nd edn, (New York : Wiley) (1970)

[17] D Rapp *Quantum Mechanics* (New York Holt, Rinehart and Winston) (1971)

[18] L I Schiff *Quantum Mechanics*, 3rd ed McGraw-Hill, New York, 1968

[19] J J Sakurai Advanced *Quantum Mechanics* (Reading, Mass Addison-Wesley) (1967)

[20] N F Mott and H S W Massey *The Theory of Atomic Collisions*, 3rd edn, (Oxford . Clarendon) (1965)

[21] B H Bransden *Atomic Collision Theory*, 2nd edn, (Menlo Park, Calif . Benjamin-Cummings) (1983)

[22] C J Joachain *Quantum Collision Theory*, 3rd edn, (Amsterdam North-Holland) (1987)

[23] H S W Massey and H B Gilbody *Electronic and Ionic Impact Phenomena*, 2nd edn, **Vol IV** (London Oxford University Press) (1974)

[24] P G Burke *Potential Scattering in Atomic Physics* (New York Plenum) (1977)

[25] J P Coleman *Case Stud At. Collision Physics*, **1** 99 (1969)

[26] M R C McDowell and J P Coleman *Introduction to the Theory of Ion-Atom Collision* (Amsterdam · North-Holland) (1970)

[27] R J Drachman and A Temkin *Case Stud At Collision Phys* **2** 399 (1972)

[28] T Y Wu and T Ohmura *Quantum Theory of Scattering* (Englewood Cliffs, N J Prentice-Hall) (1962)

[29] J R Taylor *Scattering Theory* (New York · Wiley) (1972) R G Newton *Scattering Theory of Waves and Particles*, 2nd edn, (New York Springer) (1982)

[30] L S Rodberg and R M Thaler, *Introduction to Quantum Theory of Scattering* (New York Academic) (1967)

[31] S Geltman *Topics in Atomic Collision Theory* (New York Academic) (1969)

[32] R K Nesbet *Variational Methods in Electron-Atom Scattering Theory* (New York Plenum) (1980)

[33] R K Peterkop *Theory of Ionization of Atoms* (Colorado, U.S A Colorado Associated University Press) (1977)

[34] I McCarthy and E Weigold *Electron-Atom Collisions* (Cambridge, London · Cambridge University Press) (1995)

[35] Y Itikawa *Phys. Rep.* **143** 69 (1986)

[36] B H Bransden and M R C McDowell *Phys Rep* **30** 207 (1977)

[37] B H Bransden and M R C McDowell *Phys Rep* **46** 249 (1978)

[38] P G Burke and J F Williams *Phys Rep* **34** 325 (1977)

[39] H R J Walters *Phys Rep.* **116** 1 (1984)

[40] M Inokuti *Rev Mod Phys* **43** 297 (1971)

[41] B L Moiseiwitsch and S J Smith *Rev Mod Phys* **40** 238 (1968)

[42] R K Nesbet *Adv At Mol Phys* **13** 315 (1977)

[43] P G Burke *Adv At Mol Phys* **4** 173 (1968)

[44] P G Burke and D W Robb *Adv At Mol. Phys* **11** 143 (1975)

[45] G J Schulz, *Rev Mod Phys* **45** 378 (1973)

[46] N Anderson, J W Gallagher and I V Hertel *Phys Rep* **165** 1 (1988)

[47] B L Moiseiwitsch *Rep Prog Phys* **40** 843 (1977)

[48] T T Gien *Phys Rep* **160** 123 (1988)

[49] K Bartschat *Phys Rep.* **180** 1 (1989)

[50] J Callaway *Phys Rep.* **45** 130 (1978)

[51] R J W Henry and A E Kingston *Adv At Mol Phys* **25** 267 (1988)

[52] M J Seaton *Comm. At. Mol Phys* **2** 37 (1970)

[53] M J Seaton *Rep. Prog Phys.* **46** 167 (1983)

[54] I C Percival and D Richards *AAMP* **11** 2 (1975)

[55] B H Bransden and R K Janev *AAMP* **19** 2 (1983)

[56] D R Bates *Phys Rep* **35** 305 (1978)

[57] C J Joachain and F Byron *Phys Rep* **34** 233 (1977)

[58] M R Flannery and K J McCann *J Phys.* **B7** 2518 (1974)

[59] W H Miller *Adv. Chem Phys* **25** 69 (1974)
[60] H E Saraph *Comput Phys. Commun* **3** 256 (1972), *ibid* **15** 247 (1978)
[61] M A Crees, M J Seaton and P M H Wilson *Comput. Phys Commun.* **15** 23 (1978)
[62] M J Seaton *Comput Phys Commun.* **6** 247 (1974)
[63] K A Berrington, P G Burke, M Le Dourneuf, W D Robb, K T Taylor and Lan vo Ky *Comput. Phys Commun* **14** 367 (1978)
[64] R J W Henry, S P Rountree and E R Smith *Comput. Phys Commun.* **23** 233 (1981)
[65] N S Scott and P G Burke *Comput Phys Commun* **26** 419 (1982)
[66] N S Scott and K T Taylor *Comput Phys Commun* **25** 347 (1982)
[67] S N Tiwary and D K Rai *Phys Lett* **A43** 411 (1973)
[68] S N Tiwary and D K Rai *J Phys* **B8** 1109 (1975)
[69] S N Tiwary and D K Rai *J Phys* **B9** 631 (1976)
[70] S N Tiwary and D K Rai *J Chem Phys* **68** 2427 (1978)
[71] S N Tiwary and D K Rai *Indian J Pure Appl Phys* **16** 442 (1978)
[72] S N Tiwary *Indian J Pure Appl Phys* **16** 1003 (1978)
[73] S N Tiwary and P N Chatterjee *Physica* **C 93** 285 (1978)
[74] S N Tiwary *J Phys* **B14** 2951 (1981)
[75] S N Tiwary *J Phys* **B16** L459 (1983)
[76] F H M Faisal and S N Tiwary V Deutsche *Phys Gesel* **29** 597 (1980)
[77] S N Tiwary *Physica* **C 123** 125 (1983)
[78] S N Tiwary *Chem Phys Lett* **97** 222 (1983)
[79] S N Tiwary *J Phys* **B16** L247 (1983)
[80] S N Tiwary *Phys. Rev* **A 28** 751 (1983)
[81] S N Tiwary, J Macek and D H Madison *Phys Rev* **A 32** 2541 (1985)
[82] S N Tiwary *Phys Rev* **A 32** 627 (1985)
[83] S N Tiwary *Chem Phys Lett* **116** 333 (1985)
[84] S N Tiwary *Pramana· J Phys* **35** 89 (1990)
[85] S N Tiwary *Fizika* **1** 181 (1992)
[86] A W Weiss *AAMP* **9** 1 (1973)
[87] S N Tiwary *Chem Phys Lett* **93** 47 (1982)
[88] A Hibbert, A E Kingston and S N Tiwary *J Phys* **B:15** L643 (1982)
[89] S N Tiwary *Chem Phys Lett.* **96** 333 (1983)
[90] S N Tiwary, A E Kingston and A Hibbert *J Phys* **B:16** 2457 (1983)
[91] S N Tiwary *Astrophys J* **269** 803 (1983)
[92] S N Tiwary *Astrophys J* **272** 781 (1983)
[93] S N Tiwary, P G Burke and A E Kingston *ICPEAC* (Berlin, West Germany) (1983)
[94] S N Tiwary *Proc Indian Acad Sci* **93** 1345 (1984)
[95] S N Tiwary *Invited Talk* (World Book Publisher, New York :) (1987)
[96] A E Kingston, A Hibbert and S N Tiwary *J Phys* **B:20** 3907 (1987)
[97] S N Tiwary, A P Singh, D D Singh and R J Sharma *Can J Phys.* **66** 405 (1988)
[98] S N Tiwary and G Dujardin *Symposium on Auger Process* (Paris) (1989)
[99] S N Tiwary and P Kumar *Acta Phys. Pol* **80** 23 (1991)
[100] S N Tiwary *Int J Theor Phys* **30** 825 (1991)
[101] S N Tiwary *Nuovo Cim.* **D13** 1073 (1991)
[102] S N Tiwary and D D Singh *Nuovo Cim.* **D14** 739 (1992)
[103] S N Tiwary, M Kumar, D D Singh and P Kumar *Nuovo Cim* **D15** 77 (1993)
[104] S N Tiwary, P Kandpal and A Kumar *Nuovo Cim.* **D15** 1181 (1993)

[105] S N Tiwary and P Kandpal *Nuovo Cim.* **D16** 339 (1994)
[106] S N Tiwary and B Kumar *Nuovo Cim* **D17** 393 (1995)
[107] S N Tiwary and M Kumar *Ind J Phys* **B69** 133 (1995) ; S N Tiwary *Nuovo Cim Review* **18** 1 (1995)
[108] E P Wigner *Phys Rev.* **70** 15 (1946)
[109] P G Burke, A Hibbert and W D Roob *J Phys* **B:4** 153 (1971)
[110] P G Burke, C J Noble and P Scott *Proc Roy Soc* **A410** 289 (1987)
[111] P H Norrington and I P Grant *J Phys.* **B:14** L261 (1981)
[112] U Thumm and D W Norcross *Phys Rev* **A45** 6349 (1992)
[113] S M Younger *Phys Rev.* **A22** 111 (1980)
[114] S M Younger *Quant Spectrosc Radiat Transfer* **26** 329 (1981)
[115] S S Tayal and R J W Henry *Phys Rev* **A42** 1831 (1990)
[116] A Muller, G Hofmann, K Tinschert and E Salzborn *Phys Rev Lett* **61** 1352 (1988)
[117] S R Lorentz and T M Miller *unpublished* (1991)
[118] S K Srivastava and L Vuskovic *J Phys* **B:13** 2633 (1980)
[119] L J Allen, M J Brunger, I E McCarthy and P J O Teubner *J Phys* **B:20** 4861 (1987)
[120] P J O Teubner, S J Buckman and C J Noble *J. Phys* **B:11** 2345 (1978)
[121] I Bray, D A Konovalov and I E McCarthy *Phys Rev* **A44** 7179 (1991)
[122] P J O Teubner, J L Rilley, M J Brunger and S J Buckman *J Phys.* **B:19** 3313 (1986)
[123] S J Buckman and P J O Teubner *J Phys* **B:12** 1741 (1979)
[124] D L Moores quoted in Chen *et al* (1990) (ref [125])
[125] M H Chen, K J Reed and D L Moores *Phys Rev Lett* **64** 1350 (1990)
[126] D C Gregory, L J Wang, F W Meyer and K Rinn *Phys Rev* **A 35** 3256 (1987)
[127] N R Badnell, D C Griffin and M S Pindzola *J Phys* **B:24** L275 (1991)
[128] W Lotz *Z Phys* **220** 466 (1969)
[129] B Peart, J R A Underwood and K T Dolder *J Phys* **B:22** 2789 (1989)
[130] B Peart and K T Dolder *J Phys* **B:8** 56 (1975)
[131] U Thumm and D W Norcross *Phys Rev Lett* **67** 3495 (1991)
[132] P G Burke and J F B Mitchell *J Phys* **B:6** L161 (1973) , **B7** 214 (1974)
[133] N S Scott, K Bartschat, P G Burke, O Nagy and W B Eissner *J Phys* **B:17** 3775 (1984) , **B17** L191 (1984)
[134] E M Karule (1965) , E M Karule and R K Peterkop (1965) as given in Ref (131)
[135] P J Visconi, J A Slevin and K Rubin *Phys Rev* **A3** 1310 (1971)
[136] B Jaduszliwer and Y C Chan *Phys Rev* **A45** 197 (1992)
[137] G H Wannier *Phys Rev* **90** 817 (1953)
[138] A R P Rau *Phys Rev* **A 4** 207 (1971)
[139] R Peterkop *J Phys* **B:4** 513 (1971)
[140] L Rosenberg *Phys Rev* **D 8** 1833 (1973)
[141] M R H Rudge and M J Seaton *Proc Roy Soc* **283** 262 (1965)
[142] M R H Rudge *Rev Mod Phys* **40** 564 (1968)
[143] R Peterkop *Phys Lett* **A 62** 81 (1977)
[144] F W Byron and C J Joachain *Phys Rev* **164** 1 (1967)
[145] T A Carlson *Phys Rev* **156** 142 (1967)
[146] D M P Holland, K Codling, J B West and G V Marr *J Phys* **B:12** 2465 (1979)
[147] V Schmidt, N Sander, H Kuntzmueller, P Dhez, F Wulleumier and E Kaelline *Phys Rev* **A 13** 1748 (1976)
[148] G R Wight and M J Van der Wiel *J Phys* **B:9** 1319 (1976)
[149] R L Brown *Phys Rev* **A 1** 586 (1970)

[150] M Ya Amusia, E G Drukarev, V G Gorshkov and M P Kazachkov *J Phys* **B:8** 1248 (1975)

[151] E G Drukarev *Phys Rev* **A 51** R2684 (1995)

[152] M S Yurev *Opt Spectrosc.* **38** 4 (1975)

[153] S M Varnavshik and L N Labzovskii *Opt. Spectrosc.* **47** 24 (1979)

[154] S N Tiwary *J Phys* **B:15** L323 (1982)

[155] S N Tiwary *ICPEAC* (Berlin, West Germany) (1983)

[156] S N Tiwary and G Dujardin *ICPEAC* (New York, USA) (1989)

[157] S N Tiwary *Third European Conference on Atomic and Molecular Physics* (University of Bordeaux I) (1989)

[158] S N Tiwary *ICTP LAMP* Series Report (Trieste, Italy) (1991)

[159] S L Carter and H P Kelly *Phys Rev* **A24** 170 (1981)

[160] C Pan and H P Kelly *J Phys* **B:28** 5001 (1995)

[161] G C King, M Zabek, P M Rutter, F H Read, A A McDowell, J B West and D M P Holland *J Phys* **B:21** L403 (1988)

[162] G Dawber, L Avaldi, A G McConkey, H Rojas, M A McDonald and G C King *J Phys* **B:28** L271 (1995)

[163] J M Bizau and F J Wuilleumier *J Electron Spectrosc Relat Phenom* **71** 205 (1995)

[164] J B Donahue, P A M Gram, M V Hynes, R W Hamm, C A Fost, H C Brynt, K B Butterfield, D A Clark and W W Smith *Phys Rev Lett* **48** 1538 (1982)

[165] G Dujardin, M J Besnard, L Hellner and Y Malinovitch *Phys Rev* **A 35** 5012 (1987)

[166] H Le Rouzo *Phys Rev* **A 37** 1512 (1988)

[167] A R P Rau *J Phys* **B:9** L283 (1976)

[168] A R P Rau *Opt Soc Am* **B4** 784 (1987)

[169] C H Green and A R P Rau *J Phys* **B:16** 99 (1983)

[170] H Klar and W Schlect *J Phys* **B:9** 1699 (1976)

[171] H Klar *J Phys* **B:14** 3255 (1981)

[172] J M Feagin *J. Phys* **B:17** 2433 (1984)

[173] A Temkin *Electronic and Atomic Collisions*, eds J Eichler, I V Hertel and N Stolterhoft (Amsterdam . Elsevier) (1984)

[174] A Temkin *Phys Rev Lett* **49** 365 (1982)

[175] A D Stauffer *Phys Lett* **A91** 114 (1982)

[176] D S F Crothers *J Phys* **B:19** 463 (1986)

[177] S Cjevanovic and F H Read *J Phys* **B:7** 1841 (1974)

[178] F H Read *J Phys.* **B:17** 3965 (1984)

[179] F H Read *Electron Impact Ionization*, eds T D Mark and D H Dunn (Berlin Springer) (1985)

[180] P Lablanquie, J H D Eland, I Nenner, P Morin, J Delwiche and M J Hubin-Franskin *Phys Rev Lett* **58** 992 (1987)

[181] H Kossmann, V Schmidt and T Anderson *Phys Rev. Lett* **60** 1266 (1988)

[182] P Hammond, F H Read, S Cvejanovic and G G King *J. Phys* **B:18** L141 (1985)

[183] S Spence *Phys Rev.* **A 11** 1539 (1975)

[184] P Selles, A Huetz and J Mazeau *J. Phys* **B:20** 5195 (1987)

[185] A Huetz, P Selles, D Waymel and J Mazeau *J. Phys* **B:24** 1917 (1991)

[186] P Lablanquie, J Mazeau, L Andric, P Selles and A Huetz *Phys. Rev Lett* **74** 2192 (1995)

[187] V Schmidt, *Rep. Prog Phys.* **55** 1483 (1992), *Proc. of the Workshop on Double Photoionization of He.* Publication No **ANL/PHY-94/1** (Argonne National Laboratory, Argonne, IL) (1994)

[188] O Schwarzkopf and V Schmidt *J. Phys.* **B:28** 2847 (1995)

[189] M Biagini *Phys. Rev* **A46** 656 (1992)

[190] O Schwarzkopf, B Kraessig, J Elmiger and V Schmidt *Phys. Rev. Lett* **70** 3008 (1993)

[191] P Lablanquie *Ph. D Thesis* (LURE, Orsay, France) (1989)

[192] I Nenner, P Morrin and P Lablanquie *Comm. At Mol Phys* **22** 51 (1988)

[193] J A R Samson in *Corpuscles and Radiation in Matter*, eds W Mehlhorn, *Handbuch der Physik* **Vol 32** p 23 (Berlin . Springer) (1982)

[194] A F Starace in *Corpuscles and Radiation in Matter*, ed W Mehlhorn , *Handbuch der Physik* **Vol 31** p. 1 (Berlin Springer) (1982)

[195] B Crasemann *Comm. At Mol Phys.* **22** 163 (1989)

[196] C O Almbladh and L Hedin in *Handbook on Synchrotron Radiation* ed E E Koch **Vol 1b** (1983)

[197] G Dawber, R I Hall, A G McConkey, M A MacDonald and G C King *J Phys* **B:27** L341 (1994)

[198] A R P Rau *Comm At Mol Phys* **14** 285 (1984)

[199] Z Teng and R Shakeshaft *Phys Rev* **A 47** R3487 (1993)

[200] D Proulx and R Shakeshaft *Phys Rev* **A 48** R875 (1993)

[201] M Pont and R Shakeshaft *Phys Rev* **A 51** R2676 (1995)

[202] M Pont and R Shakeshaft *J Phys* **B:28** L571 (1995)

[203] F Maulbetsch, J S Briggs, M Pont and R Shakeshaft *J Phys* **B:28** L341 (1995)

[204] M Pont, R Shakeshaft, F Maulbetsch and J S Briggs *Phys Rev* **A 53** 3671 (1996)

[205] J A R Samson, R J Bartlett and Z X He *Phys Rev* **A 46** 7277 (1992)

[206] J A R Samson in *Many-Body Theory of Atomic Structure and Photoionization*, ed T N Chang (Singapore World Scientific) (1992)

[207] J A R Samson, C H Greene and R J Bartlett *Phys Rev* **A 71** 201 (1993)

[208] R J Bartlett, P J Walsh, Z X He, Y Chung, E M Lee and J A R Samson *Phys Rev* **A 46** 5574 (1992)

[209] J A R Samson *Phys Rev Lett* **65** 2861 (1990) , J Berkowitz *Photoabsorption, Photoionization and Photoelection Spectroscopy* (New York Academic) (1979)

[210] P L Altick *Phys Rev.* **A 21** 1381 (1980)

[211] P L Altick *Phys Rev* **A 25** 128 (1982)

[212] P L Altick *J Phys* **B:16** 3543 (1983)

[213] C Garibotti and J E Miraglia *Phys Rev* **A 21** 572 (1980)

[214] M Brauner, J S Briggs and H Klar *J Phys* **B:22**, 2265 (1989)

[215] V Schmidt *Appl Opt* **19** 4080 (1980)

[216] A F Starace *Appl Opt* **19** 4051 (1980)

[217] U Fano *Rep Prog Phys* **46** 97 (1983)

[218] A Dalgarno and H R Sadeghpour *Phys. Rev* **A 46** R3591 (1992)

[219] T T Scholz, H R J Walters, P G Burke and M P Scott *Mon Not R Astr Soc* **242** 692 (1990)

[220] F Maulbetsch and J S Briggs *Phys. Rev Lett* **68** 2004 (1992)

[221] U Becker and D A Shirley *Phys. Scr* **T31** 56 (1990)

[222] R Wehlitz, F Heiser, O Hemmers, B Langer, A Menzel and U Becker *Phys Rev. Lett.* **67** 3764 (1991)

[223] J C Levin, D W Lindle, N Keller, R D Miller, Y Azuma, N B Mansour, H G Berry and I A Sellin *Phys. Rev Lett* **67** 968 (1991)

[224] J C Levin, D W Lindle, N Keller, R D Miller, Y Azuma, N B Mansour, H G Berry and I A Sellin *Phys Rev* **A 47** 16 (1993)

[225] P Lablanquie, K Ito, P Morrin, I Nenner and J D Eland *Z Phys* **D 16** 77 (1990)

[226] G Wendin *Comm At. Mol. Phys.* **17** 115 (1986)

[227] G Wendin *Photoionization of Atoms and Molecules, Proc of the Daresbury one-day Meeting on Photoionization of Atoms and Molecules*, Report **DL/SCI/R11** ed. B D Buckley (1978)

ABOUT THE REVIEWER

S. N. Tiwary

Dr. S. N. Tiwary, Professor of Physics, University Department of Physics, BRA Bihar University, Muzaffarpur, has published about 100 papers and guided several Ph.D. students. Dr. Tiwary has also published a Review Article on Atomic Structure in 1995. He is also involved in completing his Book on Quantum Physics of Atoms, Molecules and Lasers. He has worked in several countries in many capacities, *e.g.*, Associate Member, ICTP, Trieste, Italy, Alexander von Humboldt Fellow, Germany, Adjunct Professor in USA, University of Paris-Sud, CNRS Lab., Orsay, Paris, France, National Hellenic Research Foundation, Athens, Greece. He was also awarded UGC Major Research Project. Dr. Tiwary is currently interested in CI, MCHF, MCDF, R-matrix calculations in Atoms and Ions.